Nonlocal M-component nonlinear Schrödinger equations: Bright solitons, energy-sharing collisions, and positons

Jiguang Rao,[1,2] Jingsong He,[1,*] T. Kanna,[3] and Dumitru Mihalache[4]

[1]*Institute for Advanced Study, Shenzhen University, Shenzhen, Guangdong 518060, People's Republic of China*

[2]*Key Laboratory of Optoelectronic Devices and Systems of Ministry of Education and Guangdong province, College of Optoelectronic Engineering, Shenzhen University, Shenzhen, Guangdong 518060, People's Republic of China*

[3]*Nonlinear Waves Research Lab, PG and Research Department of Physics, Bishop Heber College, Thiruchirappalli - 620 017, Tamil Nadu, India*

[4]*Horia Hulubei National Institute of Physics and Nuclear Engineering, P.O. Box MG–6, Magurele, RO-077125, Romania*

(Received 22 June 2020; accepted 11 August 2020; published 1 September 2020)

The general set of nonlocal M-component nonlinear Schrödinger (nonlocal M-NLS) equations obeying the $\mathcal{PT}$-symmetry and featuring focusing, defocusing, and mixed (focusing-defocusing) nonlinearities that has applications in nonlinear optics settings, is considered. First, the multisoliton solutions of this set of nonlocal M-NLS equations in the presence and in the absence of a background, particularly a periodic line wave background, are constructed. Then, we study the intriguing soliton collision dynamics as well as the interesting positon solutions on zero background and on a periodic line wave background. In particular, we reveal the fascinating shape-changing collision behavior similar to that of in the Manakov system but with fewer soliton parameters in the present setting. The standard elastic soliton collision also occurs for particular parameter choices. More interestingly, we show the possibility of such elastic soliton collisions even for defocusing nonlinearities. Furthermore, for the nonlocal M-NLS equations, the dependence of the collision characteristics on the speed of the solitons is analyzed. In the presence of a periodic line wave background, we notice that the soliton amplitude can be enhanced significantly, even for infinitesimal amplitude of the periodic line waves. In addition to these solutions, by considering the long-wavelength limit of the obtained soliton solutions with proper parameter constraints, higher-order positon solutions of the nonlocal M-NLS equations are derived. The background of periodic line waves also influences the wave profiles and amplitudes of the positons. Specifically, the positon amplitude can not only be enhanced but also be suppressed on the periodic line wave background of infinitesimal amplitude.

DOI: 10.1103/PhysRevE.102.032201

I. INTRODUCTION

Multiple coupled nonlinear Schrödinger (CNLS) equations are a class of versatile nonlinear systems that appear in a wide scope of research fields, spanning from atomic condensates [1–4] to water waves [5], nonlinear optics [6–9], biophysics [10], and plasma physics [11]. In particular, a set of multiple CNLS equations is used to describe short-pulse propagation in multimode fibers [12] and in fiber arrays [13]. In general, these multiple CNLS equations are nonintegrable. However, some of their variants can become integrable for particular parametric choices that are of physical interest [14,15]. The interesting experiments on the coherent [16] and incoherent [17] beam propagation in photorefractive media, which can exhibit high nonlinearity even with extremely low optical power, experimental observation of the Manakov solitons [18] and dark rogue waves [19] in optical waveguides lead to a sustained intense study of integrable as well as nonintegrable CNLS systems. Such CNLS equations find numerous physical applications, for example, in wavelength division multiplexing high-bit-rate communication systems [20], multichannel bit-parallel wavelength optical fiber networks [21], and ultrashort pulse propagation in multimode fibers [22].

On the other hand, over the past two decades, the study of parity-time ($\mathcal{PT}$) symmetry has attracted considerable interest in various branches of physics because it provides strong mathematical and physical insights to the underlying dynamical system. In their seminal works [23,24], Bender and Boettcher reported a surprising finding that, although the Hamiltonian is non-Hermitian, it can possess real energy eigenvalues if it obeys $\mathcal{PT}$ symmetry. Ultimately, the fascinating properties of $\mathcal{PT}$-symmetric systems find numerous applications in the frontier topics like nonlinear optics, quantum field theory, photonics, and Bose-Einstein condensates. Particularly, the concept of $\mathcal{PT}$ symmetry has attained significant developments in optics because it can act as a fertile playground for realizing $\mathcal{PT}$-symmetric physical settings. In the realm of linear optics, complex-valued $\mathcal{PT}$-symmetric potentials have been studied in Refs. [25,26], followed by several experimental works on different optical systems, including coupled waveguide systems [27] and synthetic materials [28].

Being motivated by the theoretical and experimental studies of $\mathcal{PT}$ symmetry and the diverse applications of the

*hejingsong@szu.edu.cn; jshe@ustc.edu.cn

famous nonlinear Schrödinger (NLS) equation, Ablowitz and Musslimani [29] introduced in 2013 the following nonlocal NLS equation:

$$0 = iu_t(x,t) + u_{xx}(x,t) \pm 2V(x,t)u(x,t),$$
$$V = u(x,t)u^*(-x,t), \tag{1}$$

by employing a novel reduction of the well-known Ablowitz-Kaup-Newell-Segur (AKNS) system [30]. In Eq. (1), "$*$" denotes complex conjugation. Equation (1) contains a self-induced potential V that fulfils the $\mathcal{PT}$-symmetry condition $V^*(-x,t) = V(x,t)$. Following this pioneering work, the nonlocal NLS equation (1) has been intensively studied, and its integrable properties as well as solution dynamics have been investigated from different points of view. The sophisticated inverse scattering transform scheme for the system (1) has been developed to obtain soliton solutions with nonzero boundary conditions [29,31–34]. A hierarchy of nonlocal NLS equations that are completely integrable with long-time asymptotic behavior of the solution obeying decaying boundary conditions are found in Ref. [35]. Exact solitons, breathers, and rogue-wave solutions of Eq. (1) have been obtained by different analytical methods [29,31,32,36–51], thereby exploring their dynamical features. Furthermore, a connection between nonlocal and local NLS equations is obtained through a variable transformation [52]. The above nonlocal NLS equation (1) is gauge equivalent to an unconventional system of coupled Landau-Lifshitz equations [53]. Additionally, several integrable multidimensional versions of Eq. (1) [54,55], and a physically significant nonlocal NLS equation related to Eq. (1) [56], have been considered.

As mentioned above, the nonlinear optical systems are promising candidates for visualizing $\mathcal{PT}$-symmetry effects. Furthermore, the multicomponent generalization of the NLS equations arise in a systematic way from the Maxwell's equations if we consider short-pulse propagation in birefringent fibers [57], multimode optical fibers [58], and partially coherent beam propagation in nonlinear media with Kerr-type nonlinearity [17], as mentioned before. Of course, for other types of nonlinearities, such as cubic-quintic, saturable, and power-law nonlinearities, similar types of multiple coupled nonlinear evolution equations appear. Apart from these canonical integrable CNLS-type equations, a lot of M-component nonlinear Schrödinger (M-NLS) equations that are nonintegrable, with instantaneous nonlinearities, appear in the physical settings of coupled $\mathcal{PT}$-symmetric optical waveguides [59–63] and multicore waveguide structures [64]. The next natural problem of study in this direction is to consider the following nonlocal M-component nonlinear Schrödinger (M-NLS) equations:

$$iu_t^{(\ell)}(x,t) + u_{xx}^{(\ell)}(x,t) + 2u^{(\ell)}(x,t)\sum_{k=1}^{M}\delta_k u^{(k)}(x,t)u^{(k)*}(-x,t) = 0, \tag{2}$$

where the nonlinearity coefficients δ_k are real. Equation (2) can be viewed as describing the propagation of multiple fields with $u^{(\ell)}$ being the complex envelope of the ℓth optical field in a nonlocal nonlinear optical medium with a self-induced potential $V(x,t) = \sum_{k=1}^{M}\delta_k u^{(k)}(x,t)u^{(k)*}(-x,t)$ that satisfies the $\mathcal{PT}$-symmetry condition $V^*(-x,t) = V(x,t)$. Here, x and t represent the retarded time and the normalized distance, respectively. In other physical contexts, like water waves and atomic condensates, t denotes the temporal coordinate while x represents the spatial coordinate. The above system (2) is said to be of focusing (defocusing) type if all values of δ_j take positive (negative) values. When the parameters δ_j admit mixed values, i.e., some of them take positive values while the remaining ones take negative values, then the system (2) features mixed (focusing-defocusing) nonlinearities. Indeed, the local multicomponent NLS system with all these three types of nonlinearities, namely, focusing, defocusing, and mixed types, have been well studied and several interesting features have been explored. Recently, in addition to the above integrable multicomponent nonlocal equation (2) and its local counterpart, a few other multicomponent nonlocal systems have been proposed in Ref. [65], starting from the Fordy-Kulish equations [66].

In the nonlocal M-NLS equations (2) proposed above, the evolution of the solution at location x depends not only on the local solution at x, but also on the nonlocal solution at a distant position $(-x)$. This means that the solution states at distinct locations x and $(-x)$ are correlated, a property reminiscent of quantum entanglement between pairs of quantum particles. The nonlocal M-NLS equation (1) is integrable since it possesses a Lax pair and admits an infinite number of conserved quantities [67]. Thus, Eq. (2), being a natural generalization of the corresponding standard nonlocal NLS equation (1), is expected to be an important addition to the list of integrable systems possessing potential applications in optics, in the area of matter waves in atomic condensates, in the study of water waves, etc. Regarding the nonlocal M-NLS system (2), there exist only a few works in the literature [68–72]. So far, the general bright multisoliton solutions of Eq. (2) with arbitrary M and for general nonlinear coefficients have not been reported, to the best of our knowledge, except for two- and three-soliton solutions for the coupled nonlocal NLS system with $M = 2$, $\delta_1 = 1$, $\delta_2 = 1$ and are given by cumbersome algebraic expressions [71,72]. Thus, it is worthwhile to perform a detailed and complete investigation on the dynamics of bright soliton collisions in the framework of the nonlocal M-NLS system (2). The main objective of the present work is to investigate the collision scenarios of bright solitons and positons sitting on either a zero background or on periodic line wave background. Although a number of integrable systems admits solitons on constant and on periodic line wave background, the effects of periodic line waves on soliton collisions are yet to be investigated. Besides, the positon solution was first found in the framework of the Korteweg–de Vries equation by Matveev [73], and quickly confirmed to exist in a lot of integrable systems [74–81]. We report here the exact positon solutions in the multicomponent nonlocal equations featuring a $\mathcal{PT}$-symmetric potential.

The structure of this paper is as follows: In Sec. II, we construct the general bright $2N$-soliton solutions in terms of determinants via the Kadomtsev-Petviashvili (KP) hierarchy reduction method combined with the Hirota's bilinear method. In Sec. III, we discuss the soliton collision scenarios in the absence of a background. In Sec. IV, we study soliton collision scenarios on periodic line wave background, and

discuss the role of periodic line waves in the collision process. In Sec. V, we first obtain the higher-order positon solutions on either zero background or on the periodic line wave background by taking a long-wavelength limit of the bright $2N$-soliton solution. Then we investigate the dynamics of the positon solutions on zero background and on the periodic line wave background, respectively. Our conclusions and a brief discussion of the obtained results are given in Sec. VI.

II. BRIGHT SOLITON SOLUTIONS TO THE NONLOCAL M-NLS EQUATIONS ON ZERO AND PERIODIC LINE WAVE BACKGROUNDS

In this section, we give the bright $2N$-soliton solution of the nonlocal M-NLS equations (2), with arbitrary N and M, by employing the KP hierarchy reduction combined with Hirota's bilinear method [82]. To this end, first we bilinearize the nonlocal M-NLS equations into the following forms:

$$\begin{aligned}&\left(D_x^2+iD_t\right)g^{(\ell)}(x,t)f(x,t)=0,\\ &D_x^2(f(x,t)f(x,t))=2c\sum_{j=1}^{M}\delta_j g^{(j)}(x,t)g^{(j)*}(-x,t),\end{aligned}\tag{3}$$

through a dependent-variable transformation

$$u^{(\ell)}=\frac{g^{(\ell)}(x,t)}{f(x,t)},\tag{4}$$

for $\ell=1,2,\ldots,M$, with $c=\pm1$, D is the Hirota's bilinear differential operator, and $g^{(\ell)}(x,t)$ and $f(x,t)$ are complex functions. Here the function $f(x,t)$ is subject to the following nonlocal symmetry and complex-conjugated condition:

$$f^*(-x,t)=cf(x,t).\tag{5}$$

Below, we present the general bright $2N$-soliton solutions on the zero and periodic line wave backgrounds in terms of the determinants to the nonlocal M-NLS equation (2). A detailed derivation of the bright soliton solutions is given in the Appendix.

The nonlocal M-NLS equations (2) admit the following bright $2N$-soliton solution on zero or periodic line wave backgrounds:

$$u^{(\ell)}=\frac{g^{(\ell)}(x,t)}{f(x,t)},\quad \ell=1,2,\ldots,M,\tag{6}$$

where

$$f(x,t)=|M|,\quad g^{(\ell)}(x,t)=\begin{vmatrix}M & \Phi^T\\ -\overline{\Psi}(\ell) & 0\end{vmatrix},\tag{7}$$

and the elements of the matrix M are

$$\begin{aligned}m_{s,j}&=\frac{1}{p_s+\overline{p}_j}e^{\xi_s+\overline{\xi}_j}-\sum_{\ell=1}^{M}\frac{\delta_\ell}{p_s+\overline{p}_j}e^{\eta_{s,0}^{(\ell)}+\overline{\eta}_{j,0}^{(\ell)}},\\ \xi_s&=p_sx+ip_s^2t+\xi_{s,0},\\ \overline{\xi}_j&=\overline{p}_jx-i\overline{p}_j^2t+\overline{\xi}_{j,0},\end{aligned}\tag{8}$$

for $s,j=1,2,\ldots,K$, and the superscript T represents the transpose, Φ and $\overline{\Psi}(\ell)$ are row vectors defined by

$$\Phi=(e^{\xi_1},e^{\xi_2},\ldots,e^{\xi_K}),\quad \overline{\Psi}(\ell)=\left(e^{\overline{\eta}_{1,0}^{(\ell)}},e^{\overline{\eta}_{2,0}^{(\ell)}},\ldots,e^{\overline{\eta}_{K,0}^{(\ell)}}\right),\tag{9}$$

for $\ell=1,2,\ldots,M$. The complex parameters p_s, $\xi_{s,0}$, $\overline{p}_s$, $\overline{\xi}_{s,0}$, $\overline{\eta}_{s,0}^{(\ell)}$, and $\eta_{s,0}^{(\ell)}$ obey the following two different parametric constraints for different boundary conditions:

(a) In the absence of background, the conditions are

$$\begin{aligned}&K=2N,\quad \overline{p}_\mu=p_\mu^*,\quad \overline{\eta}_{\mu,0}^{(\ell)}=\eta_{\mu,0}^{(\ell)},\quad \overline{\xi}_{\mu,0}=\xi_{\mu,0},\\ &p_{N+s}=-p_s,\quad \xi_{N+s,0}=\xi_{s,0}^*,\quad \eta_{N+s,0}^{(\ell)}=\eta_{s,0}^{(\ell)*},\end{aligned}\tag{10}$$

for $\mu=1,2,\ldots,2N$, $s=1,2,\ldots,N$.

(b) For a periodic line wave background, the constraints read

$$\begin{aligned}&K=2N+1,\quad \overline{p}_\mu=p_\mu^*,\quad \overline{\xi}_{\mu,0}=\xi_{\mu,0},\quad \overline{\eta}_{\mu,0}^{(\ell)}=\eta_{\mu,0}^{(\ell)},\\ &\overline{\xi}_{2N+1,0}=\xi_{2N+1,0}^*,\quad \overline{\eta}_{2N+1,0}^{(\ell)}=\eta_{2N+1,0}^{(\ell)*},\\ &p_{N+s}=-p_s,\quad p_{2N+1}=ip,\quad \overline{p}_{2N+1}=ip,\\ &\xi_{N+s,0}=\xi_{s,0}^*,\quad \eta_{N+s,0}^{(\ell)}=\eta_{s,0}^{(\ell)*},\end{aligned}\tag{11}$$

for $\mu=1,2,\ldots,2N$, $s=1,2,\ldots,N$, and p a real parameter.

III. SOLITON COLLISION ON ZERO BACKGROUND

In this section, we mainly consider the soliton collisions in the absence of background. Bright two-soliton solutions of the nonlocal M-NLS equation (2) can be obtained from Eq. (6) by putting $N=1$ [i.e., $K=2$ in Eq. (10)] and the parameters are satisfying the constraints given in Eq. (10). The determinant forms of functions f and $g^{(\ell)}$ can be written explicitly as

$$\begin{aligned}f&=\begin{vmatrix}m_{1,1} & m_{1,2}\\ m_{2,1} & m_{2,2}\end{vmatrix},\\ g^{(\ell)}&=\begin{vmatrix}m_{1,1} & m_{1,2} & e^{p_1x+ip_1^2t+\xi_{1,0}}\\ m_{2,1} & m_{2,2} & e^{-p_1x+ip_1^2t+\xi_{1,0}^*}\\ -e^{\eta_{1,0}^{(\ell)}} & -e^{\eta_{1,0}^{(\ell)*}} & 0\end{vmatrix},\end{aligned}\tag{12}$$

where

$$\begin{aligned}m_{1,1}&=\frac{e^{(p_1+p_1^*)x+i(p_1^2-p_1^{*2})t+2\xi_{1,0}}}{p_1+p_1^*}-\frac{\sum_{k=1}^{M}\delta_k e^{2\eta_{1,0}^{(k)}}}{p_1+p_1^*},\\ m_{1,2}&=\frac{e^{(p_1-p_1^*)x+i(p_1^2-p_1^{*2})t+\xi_{1,0}+\xi_{1,0}^*}}{p_1-p_1^*}-\frac{\sum_{k=1}^{M}\delta_k e^{\eta_{1,0}^{(k)}+\eta_{1,0}^{(k)*}}}{p_1-p_1^*},\end{aligned}$$

and $m_{2,1}=m_{1,2}^*(x,t)$, $m_{2,2}=-m_{1,1}^*(-x,t)$. This bright two-soliton solution of the nonlocal M-NLS equation (2) is characterized by $(M+2)$ arbitrary complex parameters, p_1, $\xi_{1,0}$, and $\eta_{1,0}^{(\ell)}$, $\ell=1,2,\ldots,M$. In addition to these soliton parameters, one can also tune the system parameters, namely, the nonlinearity coefficients δ_ℓ. The velocities of the two solitons are $2p_{1I}$ and $-2p_{1I}$, respectively, which indicate that the two solitons undergo head-on collisions. Here and in the following, R and I appearing in the subscript represent the real and imaginary parts of a given parameter or a function, respectively. This bright two-soliton solution is regular when the parameters fulfill $\sum_{k=1}^{M}\delta_k e^{2\theta_{kR}}\sin(2\theta_{kI})\neq0$.

To investigate the collision scenarios of the bright two-soliton solutions in the nonlocal M-NLS equation (2), first we analyze the asymptotic properties of these solitons. To this end, we assume $p_{1,R} > 0$, $p_{I,I} > 0$, and for convenience we define the right-moving soliton along the line $\widehat{\xi}_1 = x - 2p_{1I}t$ as soliton 1 and the left-moving soliton along the line $\widehat{\xi}_2 = x + 2p_{1I}t$ as soliton 2, then the bright two-soliton solution has the following asymptotic forms:

(a) Before collision ($t \to -\infty$)

Soliton 1 ($\widehat{\xi}_1 \approx 0$, $\widehat{\xi}_2 \to -\infty$):

$$u_1^{(\ell)-} \simeq c_\ell e^{-\frac{\widehat{a}+\widehat{b}+i\widehat{c}}{2}+i\overline{R}_1} \frac{\frac{1}{p_{1R}} + \frac{1}{ip_{1I}}}{\sinh\left(p_{1R}\overline{\xi}_1 + \frac{\widehat{a}-\widehat{b}-i\widehat{c}}{2}\right)}. \tag{13}$$

Soliton 2 ($\widehat{\xi}_2 \approx 0$, $\widehat{\xi}_1 \to +\infty$):

$$u_2^{(\ell)-} \simeq c_\ell^* e^{-\frac{\widehat{a}+\widehat{b}-i\widehat{c}}{2}+i\overline{R}_2} \frac{\frac{1}{p_{1R}} + \frac{1}{ip_{1I}}}{\sinh\left(p_{1R}\overline{\xi}_2 + \frac{\widehat{b}-\widehat{a}-i\widehat{c}}{2}\right)}. \tag{14}$$

(b) After collision ($t \to +\infty$)

Soliton 1 ($\widehat{\xi}_1 \approx 0$, $\widehat{\xi}_2 \to +\infty$):

$$u_1^{(\ell)+} \simeq c_\ell e^{i\overline{R}_1-\frac{\widehat{a}_0+\widehat{b}-i\widehat{c}}{2}} \frac{\frac{\sum_{k=1}^M \delta_k c_k^{*2}}{p_{1R}} - \frac{c_\ell^* \sum_{k=1}^M \delta_k |c_k|^2}{ic_\ell p_{1I}}}{\sinh\left(p_{1R}\overline{\xi}_1 + \frac{\widehat{b}-\widehat{a}_0-i\widehat{c}}{2}\right)}. \tag{15}$$

Soliton 2 ($\widehat{\xi}_2 \approx 0$, $\widehat{\xi}_1 - \to \infty$):

$$u_2^{(\ell)+} \simeq c_\ell^* e^{i\overline{R}_2-\frac{\widehat{a}_0+\widehat{b}+i\widehat{c}}{2}} \frac{\frac{\sum_{k=1}^M \delta_k c_k^2}{p_{1R}} - \frac{c_l \sum_{k=1}^M \delta_k |c_k|^2}{ic_k^* p_{1I}}}{\sinh\left(p_{1R}\overline{\xi}_2 + \frac{\widehat{a}_0-\widehat{b}-i\widehat{c}}{2}\right)}. \tag{16}$$

The auxiliary functions and quantities in the above expressions are defined by

$$\overline{R}_1 = p_{1R}x + \left(p_{1R}^2 - p_{1I}^2\right)t, \quad \overline{R}_2 = -p_{1R}x + \left(p_{1R}^2 - p_{1I}^2\right)t,$$

$$c_k = e^{\theta_k}, \quad \widehat{a} = \ln\left(\frac{p_{1R}^2 + p_{1I}^2}{p_{1R}^2 p_{1I}^2}\right), \quad e^{\widehat{b}+i\widehat{c}} = \frac{1}{p_{1R}^2}\sum_{k=1}^M \delta_k c_k^2,$$

$$\widehat{b} = \ln\left(\frac{1}{p_{1R}^2}\left|\sum_{k=1}^M \delta_k c_k^2\right|\right),$$

$$\widehat{a}_0 = \ln\left(\frac{\left|\sum_{k=1}^M \delta_k c_k^2\right|^2}{p_{1R}^2} + \frac{\left(\sum_{k=1}^M \delta_k |c_k|^2\right)^2}{p_{1I}^2}\right). \tag{17}$$

The above asymptotic analysis shows that the changes in the amplitudes of the soliton 1 and soliton 2 after collision can be related to those before collision in the ℓth component of the nonlocal M-NLS through the following relation:

$$A_j^{(\ell)+} = T_j^{(\ell)} A_j^{(\ell)-}, \quad j = 1, 2, \quad \ell = 1, 2, \ldots, M, \tag{18}$$

where $A_j^{(\ell)-}$ and $A_j^{(\ell)+}$ are the amplitudes of the jth soliton in the $u^{(\ell)}$ component before and after collision, respectively. Their expressions read as

$$T_1^{(\ell)} = \frac{\kappa_1^{(\ell)}}{\kappa_2}, \quad A_1^{(\ell)-} = \frac{\sqrt{2}|c_\ell|}{(\sqrt{b^2+c^2}-b)^{1/2}},$$

$$T_2^{(\ell)} = \frac{\widehat{\kappa}_1^{(\ell)}}{\kappa_2}, \quad A_2^{(\ell)-} = \frac{\sqrt{2}|c_\ell^*|}{(\sqrt{b^2+c^2}-b)^{1/2}}, \tag{19}$$

where

$$b = \frac{1}{p_{1R}^2}\sum_{k=1}^M \delta_k\left(c_{kR}^2 - c_{kI}^2\right),$$

$$c = \frac{2}{p_{1R}^2}\sum_{k=1}^M \delta_k c_{kR} c_{kI},$$

$$\kappa_1^{(\ell)} = \left|\frac{\sum_{k=1}^M \delta_k c_k^{*2}}{p_{1R}} - \frac{c_\ell^* \sum_{k=1}^M \delta_k |c_k|^2}{ic_\ell p_{1I}}\right|, \tag{20}$$

$$\widehat{\kappa}_1^{(\ell)} = \left|\frac{\sum_{k=1}^M \delta_k c_k^2}{p_{1R}} - \frac{c_\ell \sum_{k=1}^M \delta_k |c_k|^2}{ic_\ell^* p_{1I}}\right|,$$

$$\kappa_2 = \sqrt{\frac{1}{p_{1R}^2}\left|\sum_{k=1}^M \delta_k c_k^2\right|^2 + \frac{1}{p_{1I}^2}\left(\sum_{k=1}^M \delta_k |c_k|^2\right)^2}.$$

From the above expressions of $A_j^{(\ell)-}$, the bright two-soliton solution possesses three features: (i) $|A_1^{(\ell)-}| = |A_2^{(\ell)-}|$ indicates that the bright two-soliton solution possesses equal amplitudes before collision in each component, which may be the result of the parameter constraint defined in Eq. (10). (ii) $|A_1^{(\ell)-}|$ and $|A_2^{(\ell)-}|$ are independent of the parameter p_{1I}, and the velocities of the two solitons are $\pm 2p_{1I}$, hence the velocity and amplitude of the bright two-soliton solution do not depend on each other before collision. (iii) $|A^{(\ell)-}|$ is proportional to p_{1R}, so the bright two-soliton solution has a higher amplitude with a larger value of p_{1R}. Importantly, transition amplitudes $T_j^{(\ell)}$ obey the following identity:

$$T_1^{(\ell)2} + T_2^{(\ell)2} = 2, \quad \ell = 1, 2, \ldots, M. \tag{21}$$

Since $T_j^{(\ell)} > 0$, the above identity indicates that the values of $T_j^{(\ell)}$ only admits two types of values; namely, $T_1^{(\ell)} = T_2^{(\ell)} = 1$, and $T_1^{(\ell)} > 1$, $T_2^{(\ell)} < 1$ (or $T_1^{(\ell)} < 1$, $T_2^{(\ell)} > 1$). When the transition amplitude $T_j^{(\ell)} = 1$, the collision between the bright solitons is elastic. This occurs only for parameters meeting the constraints $\frac{\kappa_1^{(\ell)}}{\widehat{\kappa}_1^{(\ell)}} = 1$. Furthermore, the bright two-soliton solution for the nonlocal M-NLS equation would reduce to the two-soliton solution of the standard nonlocal NLS equation [$M = 1$ in Eq. (2)] when $c_k = y^{(k)}c_1$, $k = 2, 3, \ldots, M$, where $y^{(k)}$ is a nonzero real constant. Indeed, $c_k = y^{(k)}c_1$ results in $u^{(k)} = y^{(k)}u^{(1)}$ and $\frac{\kappa_1^{(\ell)}}{\kappa_2} = \frac{\widehat{\kappa}_1^{(\ell)}}{\kappa_2} = 1$, which further yields $T_j^{(\ell)} = 1$. Thus the collision is purely elastic for this case as in the standard nonlocal NLS equation. Additionally, in a more general setting, the bright two-soliton solution undergoes the shape-changing (energy-exchanging or energy-sharing) collisions as $T_1^{(\ell)} > 1$, $T_2^{(\ell)} < 1$ (or $T_1^{(\ell)} < 1$, $T_2^{(\ell)} > 1$), where the amplitude of one soliton is enhanced (suppressed) after collision, while the amplitude of the remaining soliton gets suppressed (enhanced). From the expressions of the transition amplitudes $T_j^{(\ell)}$, one can infer that the nature of energy switching is also determined by the sign (strength) of the nonlinearity coefficients δ_ℓ as well as the soliton parameters p_{1R}, p_{1I}, and c_k. Additionally, the soliton 1 and soliton 2 suffer phase shifts Φ_1 and Φ_2, respectively. These phase shifts for

the bright two-soliton solution are given by the expression

$$\Phi_1 = -\Phi_2 = \widehat{b} - \frac{\widehat{a}_0 + \widehat{a}}{2} = -\frac{\ln \widehat{\lambda}}{2}, \tag{22}$$

where

$$\widehat{\lambda} = \left(1 + \frac{p_{1R}^2}{p_{1I}^2}\right)\left(1 + \frac{p_{1R}^2}{p_{1I}^2}\frac{\left(\sum_{k=1}^{M}\delta_k|c_k|^2\right)^2}{\left|\sum_{k=1}^{M}\delta_k c_k^2\right|^2}\right).$$

The phase shifts experienced by the two colliding solitons give rise to a change in the separation distance between the two solitons. The relative separation distance between the two colliding solitons before interaction is $d_{12}^{-} = \frac{\widehat{b}-\widehat{a}}{p_{1R}}$, and after interaction is $d_{12}^{+} = \frac{\widehat{a}_0-\widehat{b}}{p_{1R}}$. Thus the exact form of the change in relative reparation distance reads

$$\Delta = d_{12}^{+} - d_{12}^{-} \equiv \frac{1}{p_{1R}}\Phi_2. \tag{23}$$

To analyze soliton collision in the nonlocal M-NLS equation in detail, we consider the nonlocal 2-NLS equation [i.e., $M = 2$ in Eq. (2)] with alternate nonlinear coefficients δ_ℓ as an example. We mainly show the collision scenario and study the role of complex soliton parameters (i.e., c_ℓ and p_1) on the collision process. The transition amplitudes of the nonlocal 2-NLS equation are obtained from Eq. (21) as

$$\begin{aligned} T_1^{(1)} &= \sqrt{1 - \frac{\delta_2\gamma}{\widetilde{\kappa}_2^{(\ell)}}}, \quad T_2^{(1)} = \sqrt{1 + \frac{\delta_2\gamma}{\widetilde{\kappa}_2^{(\ell)}}}, \\ T_1^{(2)} &= \sqrt{1 + \frac{\delta_1\gamma}{\widetilde{\kappa}_2^{(\ell)}}}, \quad T_2^{(2)} = \sqrt{1 - \frac{\delta_1\gamma}{\widetilde{\kappa}_2^{(\ell)}}}, \end{aligned} \tag{24}$$

where

$$\begin{aligned} \gamma = {} & 4p_{1R}p_{1I}(c_{1R}c_{2R} + c_{1I}c_{2I})(c_{1R}c_{2I} - c_{1I}c_{2R}) \\ & \times \sum_{k=1}^{M}\delta_k\left(c_{kR}^2 + c_{kI}^2\right) \end{aligned}$$

and

$$\widetilde{\kappa}_2^{(\ell)} = |c_\ell|^2\left[p_{1I}^2\left|\sum_{k=1}^{M}\delta_k c_k^2\right|^2 + p_{1R}^2\left(\sum_{k=1}^{M}\delta_k|c_k|^2\right)^2\right]$$

is given by Eq. (20). As discussed above, the two-soliton solution of the 2-NLS equation would reduce to the two-soliton solution of the standard nonlocal NLS equation when $c_{1R}c_{2I} - c_{1I}c_{2R} = 0$. To avoid this case, we choose $c_{1R}c_{2I} - c_{1I}c_{2R} \neq 0$, $c_{1R}c_{2R} + c_{1I}c_{2I} = 0$ (i.e., $\gamma = 0$ or $T_j^{(\ell)} = 1$) in order to generate an elastic collision in the nonlocal 2-NLS equation, which will be discussed here. The phase shifts and relative separation distance are derived from Eqs. (22) and (23) as

$$\Phi_1 = -\Phi_2 = -\frac{\ln\lambda}{2}, \quad \Delta = \frac{\ln\lambda}{2p_{1R}}, \tag{25}$$

where

$$\lambda = \left(1 + \frac{p_{1R}^2}{p_{1I}^2}\right)\left(1 + \frac{p_{1R}^2}{p_{1I}^2}\frac{\left(\sum_{k=1}^{2}\delta_k|c_k|^2\right)^2}{\left|\sum_{k=1}^{2}\delta_k c_k^2\right|^2}\right).$$

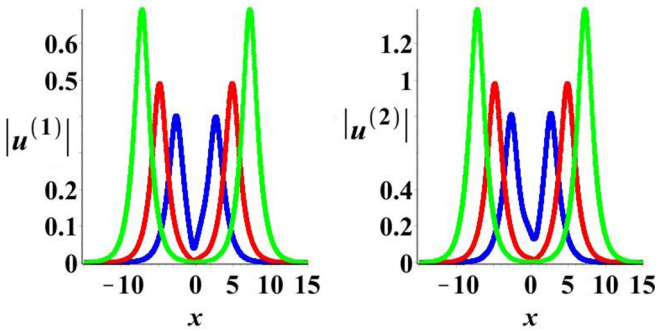

FIG. 1. The intensity profiles of bright two-soliton solution in the nonlocal 2-NLS equation with $c_1 = \frac{3}{2} + i$, $c_2 = 2 - 3i$, $p_1 = 1 + i$ and different positive nonlinear coefficients: The blue line represents the case of the positive nonlinear coefficients $\delta_1 = 3$, $\delta_2 = 3$ at time $t = -2$. The red line represents the case of the positive nonlinear coefficients $\delta_1 = 2$, $\delta_2 = 2$ at time $t = -3$. The green line represents the case of the positive nonlinear coefficients $\delta_1 = 1$, $\delta_2 = 1$ at time $t = -4$. We point out that we choose different time values to avoid soliton coincidences, so that we can better observe the corresponding intensity profiles.

In what follows, we discuss the role of nonlinear coefficients δ_1 and δ_2 in the elastic collision. As discussed above, the elastic collision occurs under parameter condition $c_{1R}c_{2I} - c_{1I}c_{2R} \neq 0$, $c_{1R}c_{2R} + c_{1I}c_{2I} = 0$. Then, the expressions of $A_j^{(\ell)}$ in Eq. (19) can be represented as

$$A^{(\ell)} = \frac{\sqrt{c_{\ell R}^2 + c_{\ell I}^2}}{(\sqrt{\widetilde{b}^2\beta^2 + \widetilde{c}^2\beta^2} - \widehat{b}\beta)^{1/2}}, \tag{26}$$

where $\widetilde{b} = \frac{c_{1I}^2}{p_{1R}^2}(c_{1R}^2 - c_{1I}^2)$, $\widetilde{c} = \frac{c_{1R}c_{1I}}{p_{1R}^2}$, $\beta = \delta_1 - \delta_2\frac{c_{2R}^2}{c_{1I}^2}$. Here we have denoted $A_j^{(\ell)+}$ and $A_j^{(\ell)-}$ as $A^{(\ell)}$ for convenience, since $A_j^{(\ell)-} = A_j^{(\ell)+}$ and $A_1^{(\ell)-} = A_2^{(\ell)-}$. For simplicity, we assume $c_{1R}^2 - c_{1I}^2 > 0$, without loss of generality, and take the absolute value of nonlinear coefficients as $|\delta_j| = \widetilde{\delta}$. The bright two-soliton solution develops singularity for $\beta = 0$. So we exclude the choice $\beta = 0$. For arbitrarily given parameters c_{1R} and c_{1I}, $A^{(\ell)}$ in Eq. (26) can be regarded as a monotonically increasing function of β when $\beta < 0$, and a monotonically decreasing function of β when $\beta > 0$. Hence, for the negative coefficients ($\delta_j = -\widetilde{\delta}$) or positive coefficients ($\delta_j = \widetilde{\delta}$), $A^{(\ell)}(\widehat{\delta}_2) > A^{(\ell)}(\widehat{\delta}_1)$ implies that larger nonlinearity generates lower soliton amplitude, where $\widehat{\delta}_1$, $\widehat{\delta}_2$ ($\widehat{\delta}_1 > \widehat{\delta}_2$) are two different values of δ. Figure 1 shows the intensity profiles of the bright two-soliton solution with different positive nonlinear coefficients. We can observe that the case of $\delta_1 = 3$, $\delta_2 = 3$ results in soliton with lower amplitude than the case of $\delta_1 = 2$, $\delta_2 = 2$ (see the blue line and red line), while the case of $\delta_1 = 2$, $\delta_2 = 2$ leads to a soliton with amplitude lesser than that of the choice $\delta_1 = 1$, $\delta_2 = 1$ (see the red line and green line). Besides, since $A^{(\ell)}(-|\beta|) < A^{(\ell)}(|\beta|)$ for any given nonzero value of β, we can obtain another two features: (i) For the mixed nonlinear coefficients, the case of $\delta_1 = \widetilde{\delta}_1$, $\delta_2 = -\widetilde{\delta}_2$ has higher soliton amplitude $A_j^{(\ell)}$ than the case of $\delta_1 = -\widetilde{\delta}_1$, $\delta_2 = \widetilde{\delta}_2$. This feature is displayed in Fig. 2, where we can see that, with the same soliton parameters c_{jR}, c_{jI} ($j = 1, 2$),

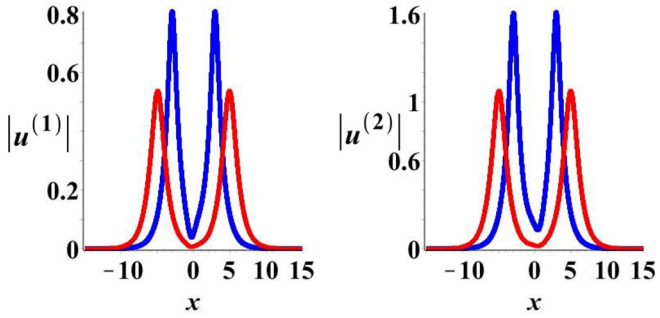

FIG. 2. The intensity profiles of bright two-soliton solution in the nonlocal 2-NLS equation with $c_1 = \frac{3}{2} + i$, $c_2 = 2 - 3i$, $p_1 = 1 + i$ and different values of mixed nonlinear coefficients: The blue line represents the case of the mixed nonlinear coefficients $\delta_1 = 1$, $\delta_2 = -1$ at time $t = -2$. The red line represents the case of the mixed nonlinear coefficients $\delta_1 = -1$, $\delta_2 = 1$ at time $t = -3$.

the mixed nonlinear coefficients $\delta_1 = 1$, $\delta_2 = -1$ (blue line) possess soliton with larger amplitude than that of the case $\delta_1 = -1$, $\delta_2 = 1$ (red line). (ii) The case of positive coefficients $\delta_j = \widetilde{\delta}_j$ results in higher soliton amplitude $A_j^{(\ell)}$ than that of negative coefficients $\delta_j = -\widetilde{\delta}_j$ when $\frac{c_{2R}^2}{c_{1I}^2} < 1$, while the case of positive coefficients gives rise to lower soliton amplitudes than that of negative nonlinear coefficients when $\frac{c_{2R}^2}{c_{1I}^2} > 1$. This feature is shown in Fig. 3, in which the blue line and red line represents the soliton amplitudes of positive coefficients

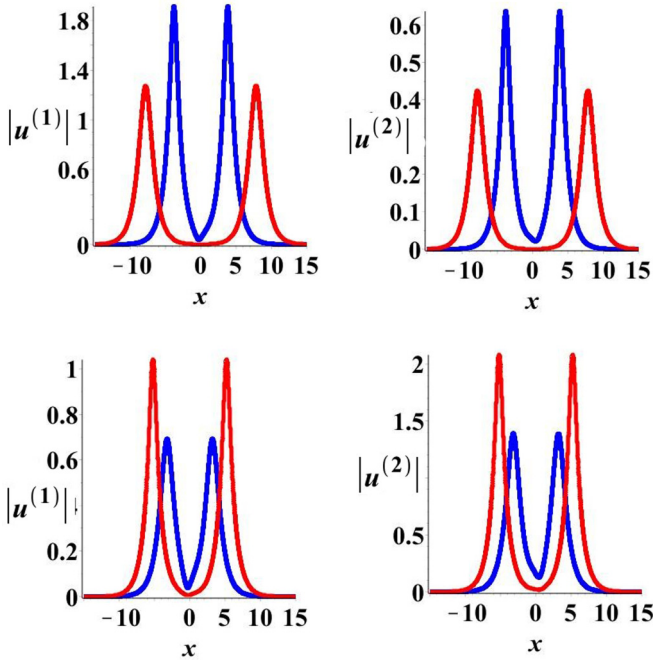

FIG. 3. The intensity profiles of bright two-soliton solution in the nonlocal 2-NLS equation with $p_1 = 1 + i$, $c_{1R} = \frac{3}{2}$, $c_{1I} = 1$: The blue line represents the case of the positive negative coefficients $\delta_1 = 1$, $\delta_2 = 1$ at $t = -2$, the red line represents the case of the negative coefficients $\delta_1 = -1$, $\delta_2 = -1$ at time $t = -4$, and with $c_{2R} = \frac{1}{3}$, $c_{2I} = -\frac{1}{2}i$ in the upper row and $c_{2R} = 2$, $c_{2I} = -3i$ in the lower row.

$\delta_j = \widetilde{\delta}_j$ and negative coefficients $\delta_j = -\widetilde{\delta}_j$, respectively. We can see that the height of the blue line is greater than that of the red line when $\frac{c_{2R}^2}{c_{1I}^2} < 1$, while it is lower for $\frac{c_{2R}^2}{c_{1I}^2} > 1$.

Below, we consider the shape-changing or energy-sharing (inelastic) collision process of bright solitons in this multicomponent nonlocal M-NLS system. To this end, we have to constrain $c_{1R}c_{2R} + c_{1I}c_{2I} \neq 0$ ($T_j^{(\ell)} \neq 1$). In this case, it is difficult to directly find the role of nonlinear coefficients δ_j on soliton amplitude $A_j^{(\ell)}$. We try to explore the role of nonlinear coefficients δ_j on the amplitude-velocity relations. Since $A_j^{(\ell)+} = A_j^{(\ell)-} T_j^{(\ell)}$ and $A_j^{(\ell)-}$ is independent of p_{1I}, and the velocity of the soliton denoted as v is $2p_{1I}$, we can discuss the relation betweens $T_j^{(\ell)}$ and v to indicate the transition amplitude-velocity relations. The transition amplitude-velocity relations can be obtained from Eq. (24) as

$$
\begin{aligned}
T_1^{(1)} &= \sqrt{1 - \frac{\delta_2 \widetilde{\gamma}}{|c_1|^2\left(\kappa_{21} v + \frac{\kappa_{22}}{v}\right)}}, \\
T_2^{(1)} &= \sqrt{1 + \frac{\delta_2 \widetilde{\gamma}}{|c_1|^2\left(\kappa_{21} v + \frac{\kappa_{22}}{v}\right)}}, \\
T_1^{(2)} &= \sqrt{1 + \frac{\delta_1 \widetilde{\gamma}}{|c_1|^2\left(\kappa_{21} v + \frac{\kappa_{22}}{v}\right)}}, \\
T_2^{(2)} &= \sqrt{1 - \frac{\delta_1 \widetilde{\gamma}}{|c_1|^2\left(\kappa_{21} v + \frac{\kappa_{22}}{v}\right)}},
\end{aligned}
\tag{27}
$$

where

$$
\begin{aligned}
\widetilde{\gamma} &= 2p_{1R}\kappa_0(c_{1R}c_{2R} + c_{1I}c_{2I}) \sum_{k=1}^{M} \delta_k \left(c_{kR}^2 + c_{kI}^2\right), \\
\kappa_0 &= c_{1R}c_{2I} - c_{1I}c_{2R}, \\
\kappa_{21} &= \frac{1}{4}\left|\sum_{k=1}^{M} \delta_k c_k^2\right|^2, \\
\kappa_{22} &= p_{1R}^2 \left(\sum_{k=1}^{M} \delta_k |c_k|^2\right)^2.
\end{aligned}
$$

To discuss the dependence of functions $T_j^{(\ell)}$ on the speed v, we assume $(c_{1R}c_{2R} + c_{1I}c_{2I})\kappa_0 > 0$ for simplicity. The behavior of functions $T_j^{(\ell)}$ by varying v, as given by Eq. (27) for different nonlinear coefficients, are listed in Table I. The table shows that (i) the functions $T_j^{(\ell)}$ of the mixed nonlinear coefficients [$\delta_1 > 0$, $\delta_2 < 0$] depend on the condition ($S > 0$ or $S < 0$) in addition to the v-dependence. Contrary to this, the positive [$\delta_1 > 0, \delta_2 > 0$] and negative nonlinearity coefficients [$\delta_1 < 0$, $\delta_2 < 0$] do not depend on the nature of S. (ii) The behavior of $T_j^{(\ell)}$ ($j, \ell = 1, 2$) is similar for positive (focusing) and negative (defocusing) nonlinearities. (iii) For the mixed nonlinear coefficients with $S < 0$, the amplitude transition $T_j^{(1)}$ has a similar dependence of v with those in the cases of positive or negative nonlinear coefficients, whereas the v dependence of $T_j^{(2)}$ is exactly opposite. The dependence of transition amplitudes of v for $S < 0$ is reversed when $S < 0$.

TABLE I. The transition amplitude-velocity behavior for $(c_{1R}c_{2R} + c_{1I}c_{2I})\kappa_0 > 0$. Here "De" denotes a decreasing function, "In" denotes an increasing function, and $S = \delta_1|c_1|^2 + \delta_2|c_2|^2$.

Velocity	Nonlinear coefficients	Parametric condition	$T_1^{(1)}$	$T_2^{(1)}$	$T_1^{(2)}$	$T_2^{(2)}$
$0 < v < \sqrt{\frac{\kappa_{22}}{\kappa_{11}}}$	$\delta_1 > 0, \delta_2 > 0$		De	In	In	De
	$\delta_1 > 0, \delta_2 < 0$	$S > 0$	In	De	In	De
		$S < 0$	De	In	De	In
	$\delta_1 < 0, \delta_2 < 0$		De	In	In	De
$v > \sqrt{\frac{\kappa_{22}}{\kappa_{11}}}$	$\delta_1 > 0, \delta_2 > 0$		In	De	De	In
	$\delta_1 > 0, \delta_2 < 0$	$S > 0$	De	In	De	In
		$S < 0$	In	De	In	De
	$\delta_1 < 0, \delta_2 < 0$		In	De	De	In

Figure 4 shows the transition amplitude-velocity relations of the bright two-soliton solutions for positive nonlinear coefficients. The blue solid lines represent soliton 1, and the red dash lines stand for soliton 2, for the two components $u^{(1)}$ (left panel) and $u^{(2)}$ (right panel). For the $u^{(1)}$ component (see left panel), $T_1^{(1)}$ (stands for soliton 1) decreases monotonically on the interval $0 < v < \sqrt{\kappa_{22}/\kappa_{21}}$ and increases monotonically on the interval $v > \sqrt{\kappa_{22}/\kappa_{21}}$, while $T_1^{(2)}$ (stands for soliton 2) increases monotonically on the interval $0 < v < \sqrt{\kappa_{22}/\kappa_{21}}$ and decreases monotonically for $v > \sqrt{\kappa_{22}/\kappa_{21}}$. $T_j^{(2)}$ have opposite behavior to those of $T_j^{(1)}$. This feature indicates that soliton 1 moving faster gains energy during the collision while it losses energy when it moves with less speed, which is in the range $0 < v < \sqrt{\kappa_{22}/\kappa_{21}}$. The reverse scenario takes place for the second soliton. Thus the velocities of the two solitons influence the energy exchange here.

In the $u^{(1)}$ component, there exists a critical value of the velocity, $v = \sqrt{\kappa_{22}/\kappa_{21}}$, at which soliton 1 (soliton 2) possesses the minimum (maximum) value for the transition amplitude value. But, for this velocity in the $u^{(2)}$ component, soliton 1 possesses maximum transition amplitude while soliton 2 has minimum value. One can also notice that the amplitude change of the two solitons in the $u^{(1)}$ component is relatively smaller than that in the $u^{(2)}$ component. Figure 5 shows the shape-changing collision of the bright two-soliton solution

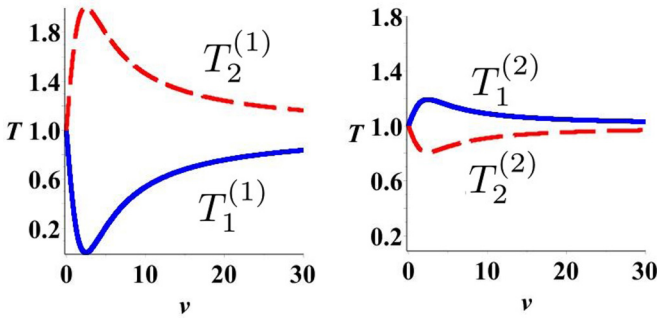

FIG. 4. The transition amplitude-velocity relations for positive nonlinear coefficients $\delta_1 = 1, \delta_2 = 1$ with parameters $p_{1I} = \frac{33}{119}\sqrt{17}$, $c_1 = 2 + i, c_2 = 1 + 5i$. The left and right panel show the amplitude-velocity relations of $u^{(1)}$ and $u^{(2)}$ components, respectively. The blue solid line stands for soliton 1 and the red dash line stands for soliton 2.

of the nonlocal 2-NLS equation (2) for focusing nonlinearity $\delta_1 = 1, \delta_2 = 1$ with $p_{1I} = \frac{33}{119}\sqrt{17}$, $c_1 = 2 + i$, $c_2 = 1 + 5i$. Here we have taken $v = \sqrt{\kappa_{21}/\kappa_{11}}$. In the $u^{(1)}$ component, the amplitudes of soliton 1 and soliton 2 before collision are 0.465, and they are 0.030 and 0.657 after collision. Thus the soliton 1 gets suppressed and the soliton 2 gets enhanced after the collision. In the $u^{(2)}$ component, the amplitudes of soliton 1 and soliton 2 before collision are 1.060, and they are 1.158 and 0.954 after collision. Thus soliton 1 gets enhanced and soliton 2 gets suppressed after collision. Hence, the shapes of the two solitons in the $u_1^{(1)}$ component changes significantly, while they alter moderately in the $u^{(2)}$ component. We note that the two solitons possess the same amplitude value before collision, which has been discussed below Eq. (20).

Figure 6 shows the shape-changing two-soliton collision in the nonlocal 2-NLS equation for negative nonlinear coefficients $\delta_1 = -1, \delta_2 = -1$ and mixed nonlinear coefficients $\delta_1 = 1, \delta_2 = -1$. It is quite interesting to note that, even for defocusing nonlinearity, one can have bright solitons in the nonlocal M-NLS system. This could be a consequence of the nonlocal and multicomponent nature of the underlying system (2). We take the soliton parameters to be the same as

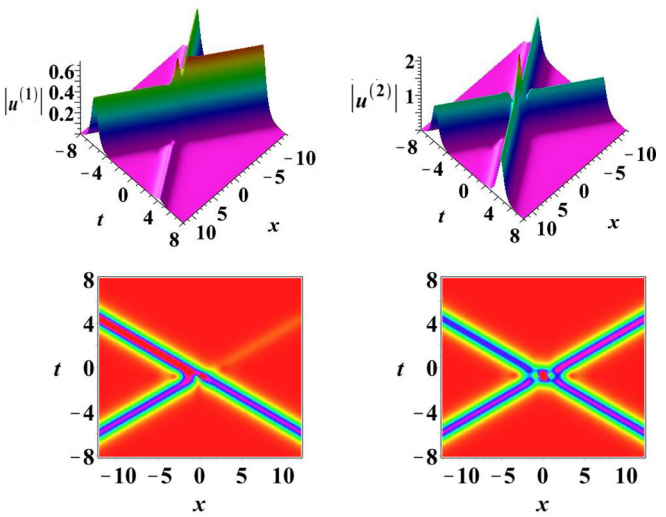

FIG. 5. The shape-changing collision of bright two solitons in the nonlocal 2-NLS equation with $\delta_1 = 1, \delta_2 = 1, p_1 = 1 + \frac{33}{119}\sqrt{17}i, c_1 = 2 + i, c_2 = 1 + 5i$.

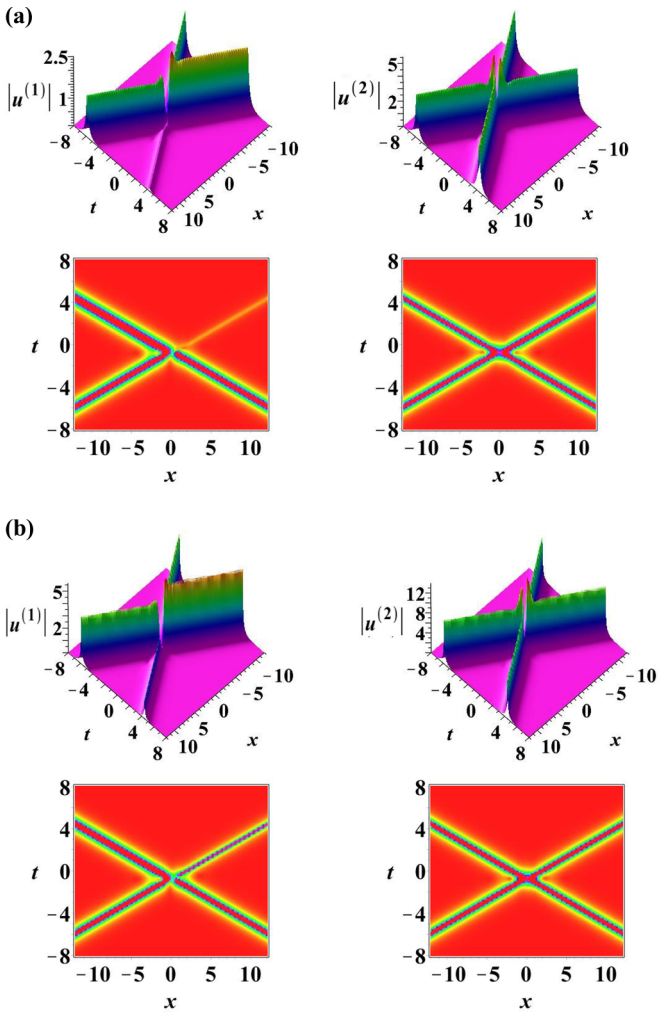

FIG. 6. The shape-changing collision of bright two solitons in the nonlocal 2-NLS equation with negative (defocusing) nonlinear coefficient ($\delta_1 = -1$, $\delta_2 = -1$, top row) and mixed nonlinear coefficients($\delta_1 = 1$, $\delta_2 = -1$, bottom row) and $p_1 = 1 + \frac{33}{119}\sqrt{17}i$, $c_1 = 2 + i$, $c_{2R} = 1 + 5i$. (a) Two-soliton collision in the 2-NLS equation with negative coefficients $\delta_1 = -1$, $\delta_2 = -1$. (b) Two-soliton collision in the 2-NLS equation with mixed coefficients $\delta_1 = 1$, $\delta_2 = -1$.

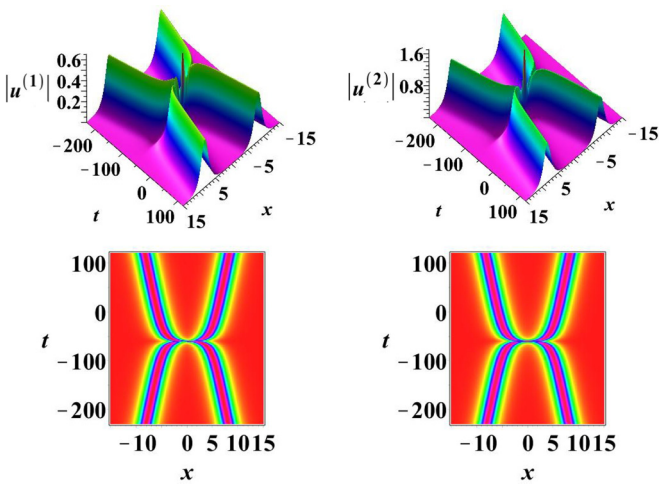

FIG. 7. The bright two-soliton solution of the nonlocal 2-NLS equation, which features the positon profile with $\delta_1 = 1$, $\delta_2 = 1$, $p_1 = 1 + 10^{-3}i$, $c_1 = 1 + i$, $c_2 = -3i$.

those in Fig. 5 except for the nonlinear coefficients. It is seen that, during the evolution process, the amplitude values of the two solitons alter. For the negative nonlinear coefficients (see the panels in the top row), the magnitudes of amplitudes of soliton 1 and soliton 2 change from 1.536 to 0.0983 and 2.170, in the $u^{(1)}$ component, respectively, and from 3.502 to 3.823 and 3.149 in the $u^{(2)}$ component, respectively. This shape-changing collision even for a defocusing nonlinearity is a special one because the local counterpart of Eq. (2) supports only an elastic collision for such a type of nonlinearity. For the mixed nonlinear coefficients (see the panels in the bottom row), the magnitude of amplitudes of soliton 1 and soliton 2 change from 3.897 to 1.560 and 5.285 in the $u^{(1)}$ component, respectively, and from 8.885 to 8.136 and 9.576 in the $u^{(2)}$ component, respectively. The intensity redistribution of the two solitons is caused by the collision, but the total amplitude values are conserved, i.e., $A_1^{(\ell)+2} + A_2^{(\ell)+2} = A_1^{(\ell)-2} + A_2^{(\ell)-2} = 2A_1^{(\ell)-2}$, where $A_j^{(\ell)-}$ represents the amplitude of the jth soliton in the ℓth component before collision, and $A_j^{(\ell)+}$ represent the amplitude of the jth soliton in the ℓth component after collision. Additionally, from Figs. 5 and 6, the magnitude of amplitudes of the two solitons before collision are affected predominantly by the nonlinear coefficients.

Apart from these, the resonant soliton is a special type of multisoliton solution, which features a localized wave that appears in the interaction regime and can be viewed as an intermediate state during soliton interaction and is different from the standard interacting solitons. Usually, the resonant solitons are achieved by appropriately choosing the soliton parameters such that the phase shift due to collision becomes infinity. Additionally, the quasiresonant soliton, a type of soliton possessing similar behavior as the resonant solitons, can be acquired by achieving the phase shifts as large as possible but within a finite regime. The present bright two-soliton solution of the nonlocal 2-NLS equation given by Eq. (12) does not support resonant solitons, since the soliton parameters do not satisfy the infinity phase shifts [i.e., $|\Phi_1| = \infty$ in Eq. (25)]. When the phase shifts are as large as possible, the bright two-soliton solution features another interesting class of soliton solutions, namely, the so-called positons that exist in several integrable systems. The localization of such positons are not along straight lines as are the conventional solitons; see Fig. 7. We investigate such particular solitons in the present nonlocal M-NLS equation (2) in Sec. V. Figure 7 shows that the particular bright two-soliton solution, which shows the wave structure of positons with parameters $\delta_1 = 1$, $\delta_2 = 1$, $p_1 = 1 + 10^{-3}i$, $c_1 = 1 + i$, $c_2 = -3i$. However, we find that the quasiresonant soliton can be obtained when the phase shifts $|\Phi_1| \to 0$, which can be realized by taking the parameters p_{1R} and p_{1I} as $\frac{p_{1R}}{p_{1I}} \ll 1$. Figure 8 shows the quasiresonant solitons, in which we can observe that the localized resonant patterns arise in the phase shift regime. The quasiresonant soliton has been studied in Ref. [72] by

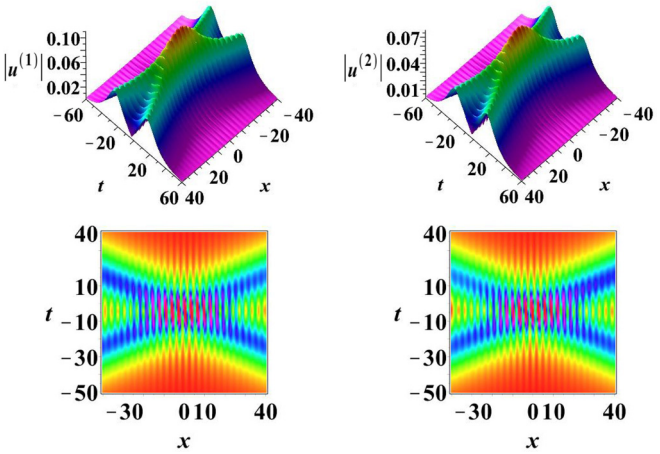

FIG. 8. The quasiresonant solitons in the nonlocal 2-NLS equation with $\delta_1 = 1$, $\delta_2 = 1$, $p_1 = \frac{1}{10} + i$, $c_1 = 1 + i$, $c_2 = -3i$.

requiring the phase shifts to be as large as possible. Here we obtain that particular soliton with phase shifts tending to zero, thus the present bright two-soliton solutions of the nonlocal 2-NLS with $\delta_1 = 1$, $\delta_2 = 1$ are different from the two-soliton solutions reported in Ref. [72].

IV. SOLITON COLLISION ON THE PERIODIC LINE WAVE BACKGROUND

In this section, we consider the solitons to be sitting on a background of periodic line waves. Actually, that type of soliton can be regarded as solitons colliding with a periodic line wave background, and the collision process results in the solitons' shape changing, and energy exchange between them and the periodic line waves. Below, we mainly discuss the bright two-soliton solution on the periodic line wave background.

The bright two-soliton solution sitting on a background of periodic line waves can be obtained from Eq. (6) with $K = 3$ [i.e., $N = 1$ in Eq. (11)] and parameters meeting the constraint condition defined in Eq. (11). The functions f and g of solutions (6) are

$$f = \begin{vmatrix} m_{1,1} & m_{1,2} & m_{1,3} \\ m_{2,1} & m_{2,2} & m_{2,3} \\ m_{3,1} & m_{3,2} & m_{3,3} \end{vmatrix},$$

$$g^{(\ell)} = \begin{vmatrix} m_{1,1} & m_{1,2} & m_{1,3} & e^{p_1 x + i p_1^2 t + \xi_{1,0}} \\ m_{2,1} & m_{2,2} & m_{2,3} & e^{-p_1 x + i p_1^2 t + \xi_{1,0}^*} \\ m_{3,1} & m_{3,2} & m_{3,3} & e^{ipx - ip^2 t + \xi_{3,0}} \\ -e^{\eta_{1,0}^{(\ell)}} & -e^{\eta_{1,0}^{(\ell)*}} & -e^{\eta_{3,0}^{(\ell)*}} & 0 \end{vmatrix}, \tag{28}$$

where the matrix elements $m_{1,1}$, $m_{1,2}$, $m_{2,1}$, and $m_{2,2}$ are given below Eq. (12), and the remaining matrix elements are

$$m_{1,3} = \frac{e^{(p_1+ip)x + i(p_1^2+p^2)t + \xi_{1,0} + \xi_{3,0}^*}}{p_1 + ip} - \frac{\sum_{k=1}^{M} \delta_k e^{\eta_{1,0}^{(k)} + \eta_{3,0}^{(k)*}}}{p_1 + ip},$$

$$m_{2,3} = \frac{e^{(-p_1+ip)x + i(p_1^2+p^2)t + \xi_{1,0}^* + \xi_{3,0}^*}}{-p_1 + ip} - \frac{\sum_{k=1}^{M} \delta_k e^{\eta_{1,0}^{(k)*} + \eta_{3,0}^{(k)*}}}{-p_1 + ip},$$

$$m_{3,1} = \frac{e^{(ip+p_1^*)x - i(p^2-p_1^2)t + \xi_{3,0} + \xi_{1,0}}}{ip + p_1^*} - \frac{\sum_{k=1}^{M} \delta_k e^{\eta_{3,0}^{(k)} + \eta_{1,0}^{(k)}}}{ip + p_1^*},$$

$$m_{3,2} = \frac{e^{(ip-p_1^*)x - i(p^2-p_1^2)t + \xi_{3,0} + \xi_{1,0}^*}}{ip - p_1^*} - \frac{\sum_{k=1}^{M} \delta_k e^{\eta_{3,0}^{(k)} + \eta_{1,0}^{(k)*}}}{ip - p_1^*},$$

$$m_{3,3} = \frac{e^{2ipx + \xi_{3,0} + \xi_{3,0}^*}}{2ip} - \frac{\sum_{k=1}^{M} \delta_k e^{\eta_{3,0}^{(k)} + \eta_{3,0}^{(k)*}}}{2ip},$$

where p is a real parameter and p_1, $\xi_{1,0}$, $\eta_{1,0}^{(\ell)}$, $\xi_{3,0}$, $\eta_{3,0}^{(\ell)}$ are complex parameters. This solution is a mixture of a bright two-soliton solution and periodic line waves, in which the two-soliton solution corresponds to Eq. (12) [or deleting the third row and the third column of determinant functions f and g in Eq. (28)] and has been investigated in Sec. II. The periodic line waves provide a periodic line wave background and can be obtained from Eq. (28) by deleting the first and the second rows and the first and second columns of the determinant expression of f and g. Before investigating the dynamics of the bright two-solitons solutions on the background of periodic line waves, we first consider the dynamical features of periodic line waves solution, which reads

$$u^{(\ell)} = \frac{2ipe^{ipx - ip^2 t + \eta_{3,0}^{(\ell)*} - \xi_{3,0}^*}}{e^{2ipx} - \sum_{k=1}^{M} \delta_k e^{\eta_{3,0}^{(\ell)} - \xi_{3,0} + \eta_{3,0}^{(\ell)*} - \xi_{3,0}^*}}, \quad l = 1, 2, \ldots, M. \tag{29}$$

This periodic solution is regular when

$$\left| \sum_{k=1}^{M} \delta_k e^{2(\eta_{3,0R}^{(\ell)} - \xi_{3,0R})} \right| > 1,$$

and whose module (i.e., $|u^{(\ell)}|$) is independent of t and the period is $\frac{2\pi}{|p|}$ along x. The amplitude of the periodic line waves is

$$|u^{(\ell)}|_p = \frac{|p| e^{\eta_{3,0R}^{(\ell)} - \xi_{3,0R}}}{\left| \sum_{k=1}^{M} \delta_k e^{2(\eta_{3,0R}^{(k)} - \xi_{3,0R})} - 1 \right|}. \tag{30}$$

The parameters in the solution given by Eq. (28) can be classified into two types: soliton parameters p_1, $\xi_{1,0}$, $\eta_{1,0}^{(\ell)}$ ($\ell = 1, 2, \ldots, M$), and periodic line wave parameters p, $\xi_{3,0}$, and $\eta_{3,0}^{(\ell)}$. The role of soliton parameters p_1, $\xi_{1,0}$, $\eta_{1,0}^{(\ell)}$ in soliton collision on zero background has been discussed in Sec. II. In the bright two-soliton collision on zero background, a typical feature is that, for a given set of parameters p_1, $\xi_{1,0}$, $\eta_{1,0}^{(\ell)}$, the amplitudes of the solitons before collision are the same [see the discussions below Eq. (20)]. However, this feature does not hold in the case of the periodic line wave background even though the amplitude of the periodic line waves is infinitesimal. To show this distinct change in the two-soliton collision in the case of the periodic line wave background comparing with that in the case of zero background, we consider the two-soliton collision on the periodic line waves whose amplitude is infinitesimal in the nonlocal 2-NLS equation [i.e., $M = 2$ in Eq. (2)]. Figure 9 shows the interaction of two solitons given by Eq. (28), with $\delta_1 = -1$, $\delta_2 = -1$ and the soliton parameters $p_1 = 1 + i$, $\xi_{1,0} = 0$, $\eta_{1,0}^{(1)} = 3$, $\eta_{1,0}^{(2)} = 10i$ in the presence of a periodic line wave background with an infinitesimal-amplitude $|u^{(\ell)}|_p = 5.153 \times 10^{-10}$ and parameters $p = \frac{1}{2}$, $\xi_{3,0} = 0$, $\eta_3^{(2)} = 10$ as well as in the absence of

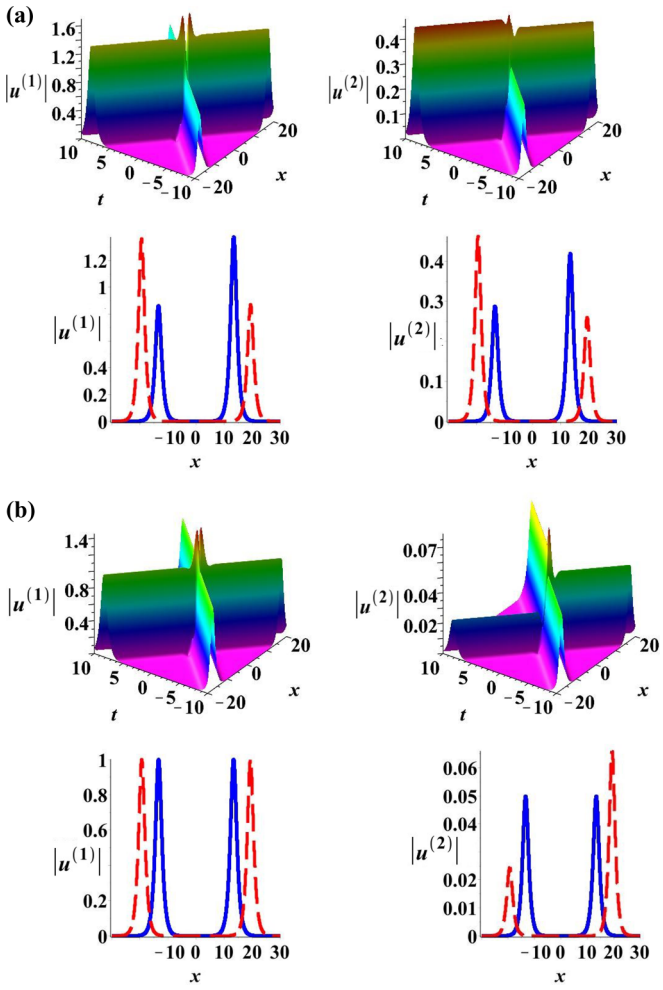

FIG. 9. The bright two-soliton solution on the infinitesimal-amplitude periodic line waves and on zero background in the nonlocal 2-NLS equation with nonlinear coefficients $\delta_1 = -1$, $\delta_2 = -1$ and $p_1 = 1 + i$, $\xi_{1,0} = 0$, $\eta_{1,0}^{(1)} = 3$, $\eta_{1,0}^{(2)} = 10i$, $p = \frac{1}{2}$, $\xi_{3,0} = 0$, $\eta_3^{(2)} = 10$. The blue solid line and red dashed line represent the intensity profiles of the bright two-soliton solution before collision ($t = -8$) and after collision ($t = 8$), respectively. (a) The two-soliton collision on the infinitesimal-amplitude periodic line wave background. (b) The two-soliton collision on zero background.

this background. One can infer from the figure that, even though the amplitude of the periodic line wave background is infinitesimal, the collision behavior of the bright two-soliton solutions on that periodic line wave background is quite different from that occurring on zero background. The corresponding differences are discussed below.

The amplitudes of the two solitons before collision are unequal even in the presence of infinitesimal-amplitude periodic line wave background [see the blue lines of the second rows of Fig. 9(a)]. But they are equal on zero background [see the blue lines of the fourth rows of Fig. 9(b)]. In the absence of background, from Eq. (19) we can obtain the amplitudes of the two solitons before and after collision in the $u^{(1)}$ and $u^{(2)}$ components as $A_1^{(1)-} = A_2^{(1)-} = 1.000\,81$, $A_1^{(1)+} = 1.001\,76$, $A_2^{(1)+} = 0.999\,87$, and $A_1^{(2)-} = A_2^{(2)-} = 0.049\,83$,

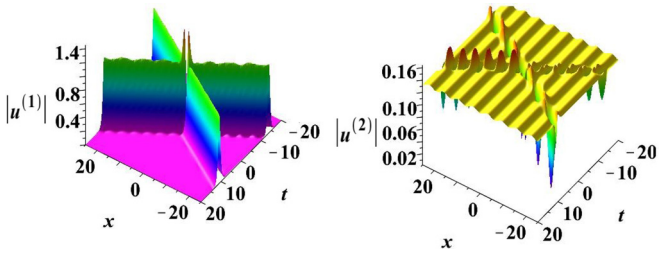

FIG. 10. The bright two-soliton solution on the periodic line wave background in the nonlocal 2-NLS equation with nonlinear coefficients $\delta_1 = -1$, $\delta_2 = -1$, periodic line waves parameters $p = -\frac{1}{2}$, $\xi_{3,0} = 0$, $\eta_{3,0}^{(1)} = -2 + 10i$, $\eta_{3,0}^{(1)} = 2 + 10i$, and the same soliton parameters as in Fig. 9.

$A_1^{(2)+} = 0.024\,510$, $A_2^{(2)+} = 0.066\,07$, where $A_j^{(\ell)-}$ and $A_j^{(\ell)+}$ denote the amplitudes of the jth soliton in the ℓth component and they satisfy $A_1^{(1)+^2} + A_2^{(1)+^2} = 2A_1^{(1)-^2} = 2A_2^{(1)-^2} \approx 2$, and $A_1^{(2)+^2} + A_2^{(2)+^2} = 2A_2^{(1)-^2} = 2A_2^{(2)-^2} \approx 0.0006$. However, for the infinitesimal-amplitude periodic line wave background, $\widetilde{A}_1^{(1)-} = 0.861\,61$, $\widetilde{A}_2^{(1)-} = 1.375\,31$, $\widetilde{A}_1^{(1)+} = 0.870\,245$, $\widetilde{A}_2^{(1)+} = 1.361\,46$, and $\widetilde{A}_1^{(2)-} = 0.287\,67$, $\widetilde{A}_2^{(2)-} = 0.420\,10$, $\widetilde{A}_1^{(2)+} = 0.260\,03$, $\widetilde{A}_2^{(2)+} = 0.462\,12$, which are obtained by numerical calculations. From these calculations, we can get $\widetilde{A}_1^{(\ell)-} \neq \widetilde{A}_2^{(\ell)-}$, and $\widetilde{A}_1^{(\ell)-2} + \widetilde{A}_2^{(\ell)-2} > 2A_2^{(\ell)-2}$, which indicates that the soliton amplitude increases on the periodic line wave background even for a very low amplitude (5.153×10^{-10}) of the periodic line waves. Besides, from $\widetilde{A}_1^{(1)-} < A_1^{(1)-}$ and $\widetilde{A}_1^{(1)-} > A_1^{(1)-}$ we obtain that the soliton on the periodic line wave background of infinitesimal-amplitude can be either enhanced or suppressed.

For the periodic line waves with larger amplitude background than that of Fig. 9 but still very small, the bright two-soliton solution on the periodic line wave background can exhibit very interesting wave patterns with the same soliton parameters as in Fig. 9. For example, with parameter choices $\xi_{3,0} = 0$, $\eta_{3,0}^{(1)} = -2 + 10i$, $\eta_{3,0}^{(2)} = 2 + 10i$, the amplitude of the periodic line waves for the $u^{(1)}$ component and $u^{(2)}$ component are $|u^{(1)}|_p = 0.002\,43$ and $|u^{(2)}|_p = 0.132\,86$, respectively. The bright two solitons on that periodic line wave background are shown in Fig. 10. In that figure, we see that the two-soliton solution in the $u^{(2)}$ component features an interesting bright-dark breather on the periodic line wave background, while the solitonic profile in the $u^{(1)}$ component does not change much, as in the case of the infinitesimal-amplitude periodic line wave background. For other periodic line wave parameters, the two-soliton solution possesses other interesting wave structures. Figure 11 shows one of them with different periodic line waves parameters and the same soliton parameters as in Fig. 9. We see that the waveforms of the two-soliton solution are quite different [see the plots of the third row of Fig. 9]. In the $u^{(1)}$ component the two-soliton solutions generate periodic localized waves, while in the $u^{(2)}$ component the two-soliton waveforms completely immerse into the periodic line wave background. Comparing Figs. 10 and 11 that were plotted for the same soliton parameters but for different types of backgrounds, we note that the characteristics of background waves play an important role

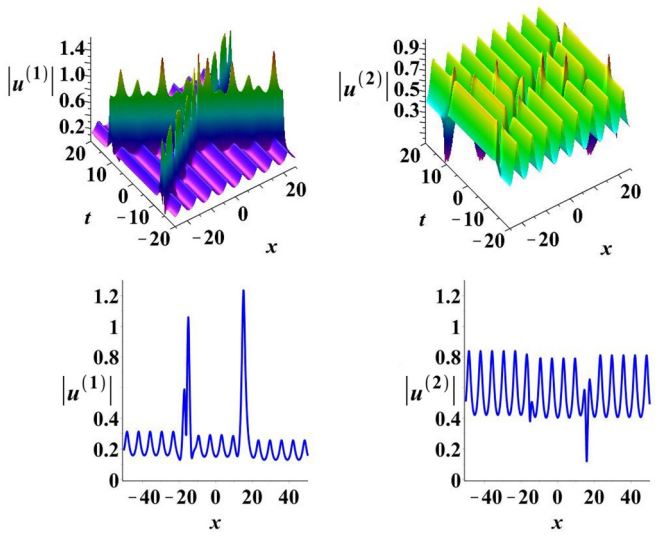

FIG. 11. The bright two-soliton solution on the finite-amplitude periodic line wave background in the nonlocal 2-NLS equation with nonlinear coefficients $\delta_1 = -1$, $\delta_2 = -1$, periodic line waves parameters $p = -\frac{1}{2}$, $\xi_{3,0} = 0$, $\eta_{3,0}^{(1)} = -\frac{1}{2} + 10i$, $\eta_{3,0}^{(1)} = \frac{1}{2} + 10i$, and the same soliton parameters as in Fig. 9. The bottom row shows the intensity profiles of the bright two-soliton waveforms on the finite-amplitude periodic line wave background at time $t = 10$.

in determining the wave profile of the solitons. Importantly, on the finite-amplitude periodic line wave background shown in Fig. 11, both the amplitude values of the two-bright soliton and the amplitude values of the periodic line waves are larger than zero (see the bottom panels in Fig. 11), an interesting result in itself. This parametric choice corresponds to zero minimum amplitude values for both the bright solitons on zero background as given in Eq. (12) and on the periodic line wave background as given in Eq. (29). However, when we consider the soliton solution on a finite-amplitude periodic line wave background as in the bottom panels of Fig. 11, the minimum amplitude values of solitons can be larger than zero. Ultimately, the collision of the bright soliton and the periodic line waves is inelastic, and energy transfer occurs between the bright two-soliton waveform and the finite-amplitude periodic line wave background. Thus in such multicomponent nonlocal setup there is a nontrivial energy exchange between the background and the propagating (as well as colliding) solitons.

V. POSITONS ON ZERO AND PERIODIC LINE WAVE BACKGROUNDS

This section is devoted to the discussion of the higher-order positon solution of the nonlocal M-NLS equation (2) on zero background and on a periodic line wave background.

A. Positons on zero background

In this section, we construct the high-order positon solution $u^{(\ell)}$ on zero background from the bright $2N$-soliton on zero background given by Eq. (6) with parameters fulfilling Eq. (10) by taking a suitable long-wavelength limit: choosing in Eq. (10) the parameters

$$e^{\xi_{s,0R}} = \widehat{\xi}_{s,0} p_{sI}, \quad e^{\eta_{s,0R}^{(\ell)}} = \widehat{\eta}_{s,0}^{(\ell)} p_{sI}, \quad \widehat{\xi}_{s,0}^2 = \sum_{k=1}^{M} \delta_k \widehat{\eta}_{s,0}^{(k)2}, \tag{31}$$

and then taking the limit as $p_{sI} \to 0$ for $s = 1, 2, \ldots, N$. By this way we can construct the high-order positon solutions of the nonlocal M-NLS equation equation.

The nonlocal M-NLS equations (2) admit the higher-order positon solution $u^{(\ell)}$ as given by Eq. (4) on zero background with

$$f = \begin{vmatrix} \widetilde{m}_{s,j} & \widetilde{m}_{s,N+j} \\ \widetilde{m}_{N+s,j} & \widetilde{m}_{N+s,N+j} \end{vmatrix},$$
$$g^{(\ell)} = \begin{vmatrix} \widetilde{m}_{s,j} & \widetilde{m}_{s,N+j} & \widetilde{\phi}_s \\ \widetilde{m}_{N+s,N+j} & \widetilde{m}_{N+s,N+j} & \widetilde{\phi}_{N+s} \\ -\widehat{\eta}_{j,0}^{(\ell)} e^{i\eta_{j,0I}^{(\ell)}} & -\widehat{\eta}_{j,0}^{(\ell)} e^{-i\eta_{j,0I}^{(\ell)}} & 0 \end{vmatrix}, \tag{32}$$

where

$$\widetilde{m}_{s,j} = \frac{\widehat{\xi}_{s,0}\widehat{\xi}_{j,0} e^{(p_{sR}+p_{jR})x + i(p_{sR}^2 - p_{jR}^2)t + i(\xi_{s,0I} + \xi_{j,0,I})}}{p_{sR} + p_{jR}} - \frac{\sum_{k=1}^{M} \delta_k \widehat{\eta}_{s,0}^{(k)} \widehat{\eta}_{j,0}^{(k)} e^{i(\eta_{s,0I}^{(k)} + \eta_{j,0I}^{(k)})}}{p_{sR} + p_{jR}},$$

$$\widetilde{m}_{s,N+j} = \frac{\widehat{\xi}_{s,0}\widehat{\xi}_{j,0} e^{(p_{sR}-p_{jR})x + i(p_{sR}^2 - p_{jR}^2)t + i(\xi_{s,0I} - \xi_{j,0,I})}}{p_{sR} - p_{jR}} - \frac{\sum_{k=1}^{M} \delta_k \widehat{\eta}_{s,0}^{(k)} \widehat{\eta}_{j,0}^{(k)} e^{i(\eta_{s,0I}^{(k)} - \eta_{j,0I}^{(k)})}}{p_{sR} - p_{jR}},$$

when $s \neq j$ and

$$\widetilde{m}_{s,N+s} = \widehat{\xi}_{s,0}^2 (x + 2ip_{s,R}t),$$
$$m_{N+s,N+j}(x,t) = -m_{s,j}^*(-x,-t),$$
$$m_{N+s,j}(x,t) = -m_{s,N+j}^*(-x,-t),$$
$$\widetilde{\phi}_s = \widehat{\xi}_{s,0} e^{p_{sR}x + ip_{sR}^2 t + i\xi_{s,0I}},$$
$$\widetilde{\phi}_{N+s} = \widehat{\xi}_{s,0} e^{-p_{sR}x + ip_{sR}^2 t - i\xi_{s,0I}}$$

for $s, j = 1, 2, \ldots, N$.

The simplest positon solution $u^{(\ell)}$ on zero background is generated by taking $N = 1$ in Eq. (32). Then the functions $g^{(\ell)}$ and f in Eq. (4) are defined by the following determinants:

$$f = \begin{vmatrix} \widetilde{m}_{1,1} & \widetilde{m}_{1,2} \\ \widetilde{m}_{2,1} & \widetilde{m}_{2,2} \end{vmatrix},$$
$$g^{(\ell)} = \begin{vmatrix} \widetilde{m}_{1,1} & \widetilde{m}_{1,2} & \widehat{\xi}_{1,0} e^{p_{1R}x + ip_{1R}^2 t + i\xi_{1,0I}} \\ \widetilde{m}_{2,1} & \widetilde{m}_{2,2} & \widehat{\xi}_{1,0} e^{-p_{1R}x + ip_{1R}^2 t - i\xi_{1,0I}} \\ -\widehat{\eta}_{1,0}^{(\ell)} e^{i\eta_{1,0I}^{(\ell)}} & -\widehat{\eta}_{1,0}^{(\ell)} e^{-i\eta_{1,0I}^{(\ell)}} & 0 \end{vmatrix}, \tag{33}$$

where

$$\widehat{m}_{1,1} = \frac{\widehat{\xi}_{1,0}^2 e^{2p_{1,R}x + 2i\xi_{1,0I}}}{2p_{1,R}} - \frac{\sum_{k=1}^{M} \delta_k \widehat{\eta}_{1,0}^{(k)2} e^{2i\eta_{1,0I}^{(k)}}}{2p_{1,R}},$$

$\widehat{m}_{1,2}(x,t) = (x + 2ip_{1,R}t)\widehat{\xi}_{1,0}^2$, $\widehat{m}_{2,1}(x,t) = -\widehat{m}_{1,2}^*(-x,-t)$, $\widehat{m}_{2,2}(x,t) = -\widehat{m}_{1,1}^*(-x,t)$.

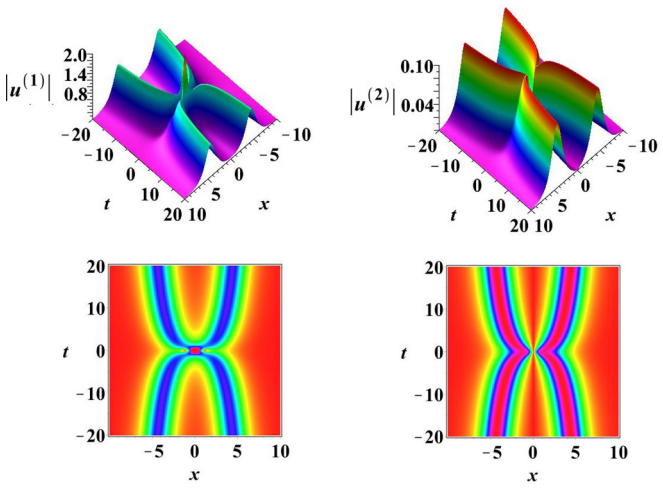

FIG. 12. The positon solution (4) of nonlocal 2-NLS equation with functions $g^{(\ell)}$ and f given in Eq. (33) with parameters $M = 2$, $\delta_1 = 1$, $\delta_2 = 1$, $p_{1R} = 1$, $\widehat{\xi}_{1,0} = \frac{\sqrt{101}}{20}$, $\widehat{\eta}^{(1)}_{1,0} = \frac{1}{2}$, $\widehat{\eta}^{(1)}_{1,0} = \frac{1}{20}$, $\xi_{1,0I} = 0$, $\eta^{(1)}_{1,0I} = \frac{\pi}{2}$, $\eta^{(2)}_{1,0I} = \frac{\pi}{20}$.

This positon solution is regular under the parameters' condition $\sum_{k=1}^{M} \delta_k \widehat{\eta}^{(k)2}_{1,0} \sin(2\eta^{(\ell)}_{1,0I} - 2\xi_{1,0I}) \neq 0$. Since this positon solution is derived from the bright two-soliton solution given in Eq. (12) with the parameter choices as given in Eq. (31) and in the soliton parameter limit $p_{1I} \to 0$, we obtain the following key properties of the positon solution from the intrinsic features of the associated bright two-soliton solution:

(i) From Eq. (19), the soliton transition amplitude $T_j^{(\ell)} = 1$ for parameter choices given by Eq. (31) and for $p_{1I} \to 0$. Thus the positon amplitude after collision stay the same as that before collision.

(ii) From Eq. (19), the positon amplitude is

$$|u^{(\ell)}|_{po} = \frac{\sqrt{2}|\widetilde{\widetilde{c}}_\ell|}{(\sqrt{\widetilde{\widetilde{b}}^2 + \widetilde{\widetilde{c}}^2} - \widetilde{\widetilde{b}})^{1/2}},$$

where

$$\widetilde{\widetilde{b}} = \frac{1}{p_{1R}^2} \sum_{k=1}^{M} \delta_k \left[\frac{\widehat{\eta}^{(k)2}_{1,0}}{\widehat{\xi}^2_{1,0}} \cos^2\left(\eta^{(k)}_{1,0I} - \xi_{1,0I}\right) - \frac{\widehat{\eta}^{(k)2}_{1,0}}{\widehat{\xi}^2_{1,0}} \sin^2\left(\eta^{(k)}_{1,0I} - \xi_{1,0I}\right) \right],$$

$$\widetilde{\widetilde{c}} = \frac{2}{p_{1R}^2} \sum_{k=1}^{M} \delta_k \frac{\widehat{\eta}^{(k)}_{1,0}}{\widehat{\xi}_{1,0}} \cos\left(\eta^{(k)}_{1,0I} - \xi_{1,0I}\right) \frac{\widehat{\eta}^{(k)}_{1,0}}{\widehat{\xi}_{1,0}} \times \sin\left(\eta^{(k)}_{1,0I} - \xi_{1,0I}\right).$$

(iii) From Eqs. (22) and (23), the positon shifts are $\Phi_1 = -\infty$ and $\Phi_2 = +\infty$, and the change in the relative reparation distance of soliton is $\Delta = +\infty$. From these properties, the positon can be regarded as two solitons possessing the same amplitudes and exhibiting elastic collision, resulting in infinite soliton shifts and infinite relative reparation distance. Figure 12 shows the positon solution of the nonlocal 2-NLS equation (2) with the parameters $M = 2$, $\delta_1 = 1$, $\delta_2 = 1$, $p_{1R} = 1$, $\widehat{\xi}_{1,0} = \frac{\sqrt{101}}{20}$, $\widehat{\eta}^{(1)}_{1,0} = \frac{1}{2}$, $\widehat{\eta}^{(1)}_{1,0} = \frac{1}{20}$, $\xi_{1,0I} = 0$, $\eta^{(1)}_{1,0I} = \frac{\pi}{2}$, $\eta^{(2)}_{1,0I} = \frac{\pi}{20}$. It is seen that, due to the collision, the wave structures of the positon in the interaction region are different in the $u^{(1)}$ component and in the $u^{(2)}$ one: the region of their intersection acquires a higher amplitude in the $u^{(1)}$ component but it does not in the $u^{(2)}$ component. The two interacting waves overlap in the interaction region in the $u^{(1)}$ component while they are completely separated in the $u^{(2)}$ component. The positon amplitude values for the $u^{(1)}$ and the $u^{(2)}$ components are $|u^{(2)}|_{po} = 1.0050$ and $|u^{(2)}|_{po} = 0.1005$, respectively.

Here we note that, in Eq. (31) the parameter condition $\widehat{\xi}^2_{1,0} = \sum_{k=1}^{M} \delta_k \widehat{\eta}^{(k)2}_{1,0}$, when $\delta_\ell < 0$ for $\ell = 1, 2, \ldots, M$, corresponds to negative (defocusing) nonlinearities for all $u^{(\ell)}$ components in Eq. (2). This shows that the positon solutions cannot exist for defocusing nonlinearities because this parameter condition cannot be satisfied. When $\delta_\ell > 0$ or $\delta_k \delta_j < 0$ ($k \neq j$ and $k, j = 1, 2, \ldots, M$), which correspond to positive nonlinear coefficients for all $u^{(\ell)}$ components in Eq. (2) or mixed nonlinear coefficients for u_k and u_j components in Eq. (2), the parameter condition can very well be satisfied. Hence the positons can exist in the nonlocal M-NLS system (2) with both focusing and mixed nonlinearities.

B. Positon on periodic line wave background

Next, we consider the positons on the periodic line wave background. By taking the same limiting procedure explained in the previous section, one can obtain the higher-order positons on the periodic line wave background. In this regard, we take the parameters as given by Eq. (31) and insert them into Eq. (11). Then by taking the limit $p_{1I} \to 0$ we obtain the higher-order positon solution on the periodic line wave background to the nonlocal M-NLS equation (2).

The nonlocal M-NLS equations (2) admit higher-order positon solution $u^{(\ell)}$ given by Eq. (4) on the periodic line wave background with functions $g^{(\ell)}$ and f defined by the following determinants:

$$f = \begin{vmatrix} \widetilde{m}_{s,j} & \widetilde{m}_{s,N+j} & \widetilde{m}_{s,2N+1} \\ \widetilde{m}_{N+s,j} & \widetilde{m}_{N+s,N+j} & \widetilde{m}_{N+s,2N+1} \\ \widetilde{m}_{2N+1,j} & \widetilde{m}_{2N+1,N+j} & \widetilde{m}_{2N+1,2N+1} \end{vmatrix},$$

$$g^{(\ell)} = \begin{vmatrix} \widetilde{m}_{s,j} & \widetilde{m}_{s,N+j} & \widetilde{m}_{s,2N+1} & \widetilde{\phi}_s \\ \widetilde{m}_{N+s,N+j} & \widetilde{m}_{N+s,N+j} & \widetilde{m}_{N+s,2N+1} & \widetilde{\phi}_{N+s} \\ \widetilde{m}_{2N+1,j} & \widetilde{m}_{2N+1,N+j} & \widetilde{m}_{2N+1,2N+1} & \widetilde{\phi}_{2N+1} \\ -\widehat{\eta}^{(\ell)}_{j,0} e^{i\eta^{(\ell)}_{j,0I}} & -\widehat{\eta}^{(\ell)}_{j,0} e^{-i\eta^{(\ell)}_{j,0I}} & -e^{\eta^{(\ell)*}_{2N+1,0}} & 0 \end{vmatrix}, \tag{34}$$

where

$$\widetilde{m}_{s,2N+1} = \frac{\widehat{\xi}_{s,0} e^{(p_{sR}+ip)x + i(p_{sR}^2+p^2)t + i\xi_{s,0I} + \xi^*_{2N+1,0}}}{p_{sR} + ip} - \frac{\sum_{k=1}^{M} \delta_k \widehat{\eta}^{(k)}_{1,0} e^{i\eta^{(k)}_{s,0I} + \eta^{(k)*}_{2N+1,0}}}{p_{sR} + ip},$$

$$\widetilde{m}_{N+s,2N+1}=\frac{\widehat{\xi}_{s,0}e^{(-p_{sR}+ip)x+i(p_{sR}^2+p^2)t-i\xi_{s,0I}+\xi^*_{2N+1,0}}}{-p_{sR}+ip}-\frac{\sum_{k=1}^{M}\delta_k\widehat{\eta}^{(k)}_{s,0}e^{-i\eta^{(k)}_{s,0I}+\eta^{(k)*}_{2N+1,0}}}{-p_{sR}+ip},$$

$$\widetilde{m}_{2N+1,j}=\frac{\widehat{\xi}_{j,0}e^{(p_{jR}+ip)x-i(p_{jR}^2+p^2)t+i\xi_{j,0I}+\xi_{2N+1,0}}}{p_{jR}+ip}-\frac{\sum_{k=1}^{M}\delta_k\widehat{\eta}^{(k)}_{j,0}e^{i\eta^{(k)}_{j,0I}+\eta^{(k)}_{2N+1,0}}}{p_{jR}+ip},$$

$$\widetilde{m}_{2N+1,N+j}=\frac{\widehat{\xi}_{j,0}e^{(-p_{jR}+ip)x-i(p_{jR}^2+p^2)t-i\xi_{j,0I}+\xi_{2N+1,0}}}{-p_{jR}+ip}-\sum_{k=1}^{M}\delta_k\widehat{\eta}^{(k)}_{j,0}e^{-i\eta^{(k)}_{j,0I}+\eta^{(k)}_{2N+1,0}}-p_{jR}+ip, \tag{35}$$

and $m_{s,j}$, $m_{s,N+j}$, $m_{N+s,j}$, $m_{N+s,N+j}$, $\widetilde{\phi}_s$, $\widetilde{\phi}_{N+s}$ are defined below Eq. (32), and $\widetilde{\phi}_{2N+1}=e^{ipx-ip^2t+\xi_{2N+1,0}}$.

The simplest positon solution on the periodic line wave background can be obtained from Eq. (34) with $N=1$, and the corresponding functions $g^{(\ell)}$ and f are given by the following determinants:

$$f=\begin{vmatrix}\widetilde{m}_{1,1} & \widetilde{m}_{1,2} & \widetilde{m}_{1,3}\\ \widetilde{m}_{2,1} & \widetilde{m}_{2,2} & \widetilde{m}_{2,3}\\ \widetilde{m}_{3,1} & \widetilde{m}_{3,2} & m_{3,3}\end{vmatrix},$$

$$g^{(\ell)}=\begin{vmatrix}\widetilde{m}_{1,1} & \widetilde{m}_{1,2} & \widetilde{m}_{1,3} & \widehat{\xi}_{1,0}e^{p_{1R}x+ip_{1R}^2t+i\xi_{1,0I}}\\ \widetilde{m}_{2,1} & \widetilde{m}_{2,2} & \widetilde{m}_{2,3} & \widehat{\xi}_{1,0}e^{-p_{1R}x+ip_{1R}^2t-i\xi_{1,0I}}\\ \widetilde{m}_{3,1} & \widetilde{m}_{3,2} & m_{3,3} & e^{ipx-ip^2t+\xi_{3,0}}\\ -\widehat{\eta}^{(\ell)}_{1,0}e^{i\eta^{(\ell)}_{1,0I}} & -\widehat{\eta}^{(\ell)}_{1,0}e^{-i\eta^{(\ell)}_{1,0I}} & -e^{\eta^{(\ell)*}_{3,0}} & 0\end{vmatrix}, \tag{36}$$

where $\widetilde{m}_{1,1}$, $\widetilde{m}_{1,2}$, $\widetilde{m}_{2,1}$, $\widetilde{m}_{2,2}$ are defined below Eq. (33), and $m_{3,3}$ is defined below Eq. (28), and

$$\widetilde{m}_{1,3}=\frac{1}{p_{1R}+ip}\left[\widehat{\xi}_{1,0}e^{(p_{1R}+ip)x+i(p_{1R}^2+p^2)t+i\xi_{1,0I}+\xi^*_{3,0}}-\sum_{k=1}^{M}\delta_k\widehat{\eta}^{(k)}_{1,0}e^{i\eta^{(k)}_{1,0I}+\eta^{(k)*}_{3,0}}\right],$$

$$\widetilde{m}_{2,3}=\frac{1}{-p_{1R}+ip}\left[\widehat{\xi}_{1,0}e^{(-p_{1R}+ip)x+i(p_{1R}^2+p^2)t-i\xi_{1,0I}+\xi^*_{3,0}}-\sum_{k=1}^{M}\delta_k\widehat{\eta}^{(k)}_{1,0}e^{-i\eta^{(k)}_{1,0I}+\eta^{(k)*}_{3,0}}\right],$$

$$\widetilde{m}_{3,1}=\frac{1}{p_{1R}+ip}\left[\widehat{\xi}_{1,0}e^{(p_{1R}+ip)x-i(p_{1R}^2+p^2)t+i\xi_{1,0I}+\xi_{3,0}}-\sum_{k=1}^{M}\delta_k\widehat{\eta}^{(k)}_{1,0}e^{i\eta^{(k)}_{1,0I}+\eta^{(k)}_{3,0}}\right],$$

$$\widetilde{m}_{3,2}=\frac{1}{-p_{1R}+ip}\left[\widehat{\xi}_{1,0}e^{(-p_{1R}+ip)x-i(p_{1R}^2+p^2)t-i\xi_{1,0I}+\xi_{3,0}}-\sum_{k=1}^{M}\delta_k\widehat{\eta}^{(k)}_{1,0}e^{-i\eta^{(k)}_{1,0I}+\eta^{(k)}_{3,0}}\right],$$

where the parameters $\xi_{3,0}$ and $\eta^{(k)}_{3,0}$ are complex, and the remaining parameters are real.

The above positon solution on a periodic line wave background is characterized by $4M+5$ arbitrary parameters containing $2M+3$ positon parameters (i.e., $\widehat{\xi}_{1,0}$, $\xi_{1,0I}$, $\widehat{\eta}^{(\ell)}_{1,0}$, $\eta^{(\ell)}_{1,0I}$, p_{1R}, $\ell=1,2,\ldots,M$) and $2M+2$ periodic line wave background parameters (i.e., $\xi_{3,0}$, $\eta^{(\ell)}_{3,0}$, p). In the following, we mainly consider the role of the periodic line background on this positon solution. For this purpose, we take the nonlocal 2-NLS equation [i.e., $M=2$ in Eq. (2)] as an example, and adopt the same positon parameters as those in Fig. 12. We study the dynamics of positons on two different types of periodic line wave backgrounds, namely, the infinitesimal-amplitude periodic line wave background and the finite-amplitude periodic line wave background. The amplitudes of periodic line wave backgrounds in the $u^{(1)}$ and $u^{(2)}$ components are $|u^{(1)}|_p=|u^{(2)}|_p=8.2446\times10^{-9}$ (which are approximately equal to zero) for the background parameters $p=-2$, $\xi_{3,0}=0$, $\eta^{(\ell)}_{3,0}=\eta^{(2)}_{3,0}=10+i$. The corresponding positon on that periodic line wave background is shown in Fig. 13, in which the periodic line wave background is visually the same as zero background in Fig. 12. However, comparing with the positon on zero background shown in Fig. 12, we note that in spite of the positon parameters being same in these two figures, their wave profiles are quite different. For the $u^{(2)}$ component, the two waves overlap in the interaction region on the infinitesimal-amplitude periodic line wave background while they are completely separated on zero background (see right panels in Figs. 12 and 13). In the interaction region, the $u^{(1)}$ component does not acquire a higher amplitude as on zero background (see left panels in Figs. 12 and 13), while the $u^{(2)}$ component attains a much higher amplitude than that in the case of zero background case (see right panels in Figs. 12 and 13). The positon amplitude of the $u^{(1)}$ component on the infinitesimal-amplitude periodic line wave background is slightly lower than that in the case of zero background, while the positon amplitude of the $u^{(2)}$ component on the infinitesimal-amplitude periodic line wave background is much higher than that in the case of zero background (see the lower panels in Fig. 13). This

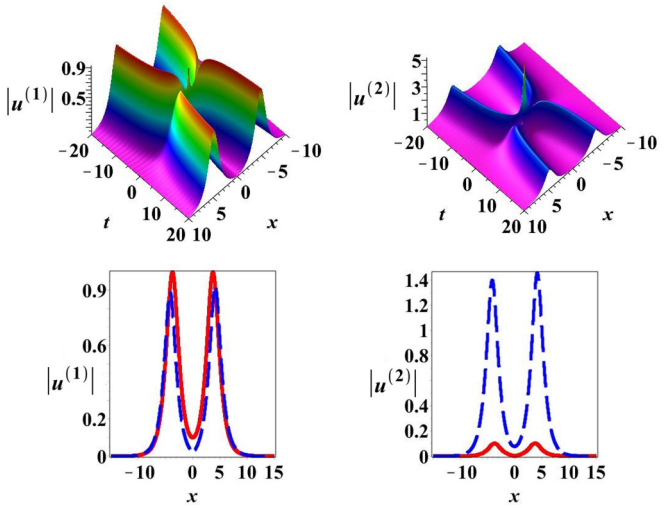

FIG. 13. The upper row shows the positon solution (4) on the infinitesimal-amplitude periodic line wave background of the nonlocal 2-NLS equation with $\delta_1 = -1$, $\delta_2 = -1$, and functions $g^{(\ell)}$ and f given in Eq. (36) and the same positon parameters as in Fig. 12 and background parameters $p = -2$, $\xi_{3,0} = 0$, $\eta_{3,0}^{(\ell)} = 10 + i$, $\eta_{3,0}^{(2)} = 10 + i$. The lower row shows the intensity profile of the positon at time $t = -10$ on the zero background shown in Fig. 12 and on the infinitesimal-amplitude periodic line wave background: the red solid line represents the intensity profile in the case of zero background, whereas the blue dashed line represents the intensity profile in the case of the infinitesimal-amplitude periodic line wave background.

demonstrates that the amplitude of the positon can not only be enhanced but also be suppressed in the presence of a periodic line wave background. It further shows that the indirect interaction in the form of a superposition of a bright soliton with periodic line waves does not always generate higher soliton amplitude in the system (2). This behavior is different from the so-far reported superposition of antidark (dark) solitons

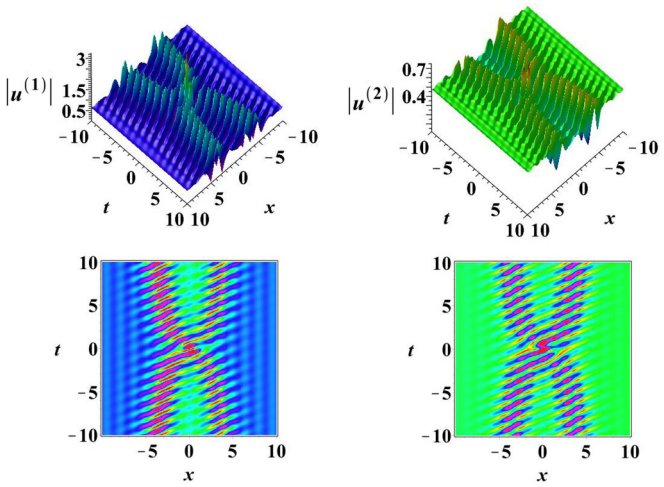

FIG. 14. The positon solution (4) on the finite-amplitude periodic line wave background of the nonlocal 2-NLS equation with $\delta_1 = -1$, $\delta_2 = -1$, and functions $g^{(\ell)}$ and f given in Eq. (33). We choose the same positon parameters as in Fig. 12 and the background parameters are $p = -2$, $\xi_{3,0} = 0$, $\eta_{3,0}^{(\ell)} = \frac{3}{2} - i$, $\eta_{3,0}^{(2)} = 1 + 2i$.

and periodic line waves, which would always generate higher (deeper) soliton amplitude [51]. Additionally, on the finite-amplitude periodic line wave background, the positon features a peculiar periodic waves structure, which is much different from that obtained in the case of an infinitesimal-amplitude periodic line wave background, shown in Fig. 13. Figure 14 shows the positon waveform on the finite-amplitude periodic line wave background with the same positon parameters as in the case of zero background (see Fig. 12) and for periodic line wave background parameters $p = -2$, $\xi_{3,0} = 0$, $\eta_{3,0}^{(\ell)} = \frac{3}{2} - i$, $\eta_{3,0}^{(2)} = 1 + 2i$. The amplitude of the periodic line wave background is $|u^{(1)}|_p = 0.458\,50$, $|u^{(2)}|_p = 0.168\,67$. It is seen that the wave profiles of the positon are quite different from those appearing in the case of zero background (see Fig. 12) or in the case of the infinitesimal-amplitude periodic line wave background (see Fig. 13).

VI. CONCLUSION

In this paper, we consider a general form of nonlocal M-component NLS equation featuring all types of nonlinearities, namely, focusing, defocusing, and mixed nonlinearities in a nonlocal physical setting and with a self-induced potential respecting $\mathcal{PT}$ symmetry. By employing the Hirota's bilinear method in conjunction with the KP hierarchy reduction procedure, bright $2N$ solitons in the absence of background and in the presence of periodic line wave background are constructed in terms of determinants. Then, by taking the long-wavelength limit of the bright two-soliton solution with proper parameter choices, positon solutions sitting on either zero background or on periodic line wave background are obtained. First, we consider the soliton collision in the M-NLS equation in the case of zero background and we identify that there exist two types of collision scenarios: elastic collision and shape-changing (inelastic) collision. To facilitate the understanding of collision features, we consider the nonlocal 2-NLS equation as an example, and we analyze the role played by the nonlinear coefficients of the nonlocal 2-NLS equation and by the soliton parameters on the interacting bright solitons. In particular, we demonstrate that the Manakov-type energy sharing collision, where the interacting bright solitons undergo a nontrivial energy redistribution along with preserving the energy in the individual components as well as the total energy, can take place in the nonlocal M-NLS system (2) even with fewer parameters. Surprisingly, such a collision takes place for the defocusing nonlinearity too, and this interesting problem has to be studied further. Also, the intricate dependence of the transition amplitudes that characterize such collisions, on the speed of the interacting solitons, is analyzed in detail. Then, we investigate the soliton collision scenarios for solitons sitting on the periodic background, and we compare the collision features with those that occur in the case of zero background. We find that, even though the amplitude of the periodic line wave background is infinitesimal, the shape of the soliton changes significantly as compared with that of the soliton sitting on zero background. The obvious difference is that the amplitudes of the two solitons before collision are equal in the case of zero background, but they are not equal in the case of the periodic line waves infinitesimal background. Another important difference is that both the minimum values

of the bright two-soliton solution on zero background and the minimum amplitude values of the periodic line waves are zero, but for the two-soliton solution on the finite-amplitude periodic line wave background, both the minimum values of the bright two-soliton waveform and the minimum amplitude values of the periodic line waves are larger than zero. Thus, energy transfer happens between the two-soliton waveform and the periodic line wave background, which induces an upward shift in the periodic background. Finally, we also construct the general higher-order positon solutions on zero background and on periodic line wave background by taking the long-wavelength limit of the $2N$-soliton solution on the corresponding background, and then we investigate the key role of the background in the collision process.

Here we have to note that general bright-bright, bright-dark, and dark-dark N-soliton solutions to the local M-NLS equation with constant background have been constructed by Feng [83] by using the Kadomtsev-Petviashvili hierarchy-reduction method in conjunction with the Hirota's bilinearization procedure.

ACKNOWLEDGMENTS

The work of J.H. was supported by the National Natural Science Foundation of China (Grant No. 11671219). The work of J.R. was supported by the Natural Science Foundation of Guangdong Province, China (Grant No. 2019A1515110208). The work of T.K. was supported by DST-SERB, Government of India, in the form of a major research project (File No. EMR/2015/001408). T.K. also thanks the Principal and Management of Bishop Heber College, Thiruchirapalli, for constant support and encouragement.

APPENDIX

In this Appendix we present the derivation of the bright $2N$-soliton solutions given in Eq. (6) to the nonlocal M-NLS equation (2) via the KP hierarchy-reduction method.

Referring to Sato theory [84–86], the bilinear equations in the multicomponent KP hierarchy

$$\begin{aligned}\left(D_{x_1}^2 - D_{x_2}\right)\tau_1(\ell)\tau_0 &= 0,\\ D_{x_1}D_{y_\ell}\tau_0\tau_0 &= -2\tau_1(\ell)\tau_{-1}(\ell),\end{aligned} \tag{A1}$$

where $\ell = 1, 2, \ldots, M$, admit the following tau functions expressed in Gram-type determinant form:

$$\begin{aligned}\tau_0 &= |M|, \quad \tau_1(\ell) = \begin{vmatrix} M & \Phi^T \\ -\overline{\Psi}(\ell) & 0 \end{vmatrix},\\ \tau_{-1}(\ell) &= \begin{vmatrix} M & \Psi^T(\ell) \\ -\overline{\Phi} & 0 \end{vmatrix},\end{aligned} \tag{A2}$$

where the elements of the matrix M are

$$m_{s,j} = \frac{1}{p_s + \overline{p}_j} e^{\xi_s + \overline{\xi}_j} + \sum_{\ell=1}^{M} \frac{1}{q_s^{(\ell)} + \overline{q}_j^{(\ell)}} e^{\eta_s^{(\ell)} + \overline{\eta}_j^{(\ell)}}, \tag{A3}$$

with

$$\begin{aligned}\xi_s &= p_s x_1 + p_s^2 x_2 + \xi_{s,0}, \quad \overline{\xi}_j = \overline{p}_j x_1 + \overline{p}_j^2 x_2 + \overline{\xi}_{j,0},\\ \eta_j^{(\ell)} &= q_j^{(\ell)} y_\ell + \eta_{s,0}^{(\ell)}, \quad \overline{\eta}_j^{(\ell)} = \overline{q}_j^{(\ell)} y_\ell + \overline{\eta}_{s,0}^{(\ell)},\end{aligned} \tag{A4}$$

for $1 \leqslant s, j \leqslant K$, K is a positive integer, the superscript T represents the transpose, and Φ, $\Psi(\ell)$, $\overline{\Phi}$, and $\overline{\Psi}(\ell)$ are row vectors defined by

$$\begin{aligned}\Phi &= (e^{\xi_1}, e^{\xi_2}, \ldots, e^{\xi_K}), \quad \Psi(\ell) = \left(e^{\eta_1^{(\ell)}}, e^{\eta_2^{(\ell)}}, \ldots, e^{\eta_K^{(\ell)}}\right),\\ \overline{\Phi} &= (e^{\overline{\xi}_1}, e^{\overline{\xi}_2}, \ldots, e^{\overline{\xi}_K}), \quad \overline{\Psi}(\ell) = \left(e^{\overline{\eta}_1^{(\ell)}}, e^{\overline{\eta}_2^{(\ell)}}, \ldots, e^{\overline{\eta}_K^{(\ell)}}\right),\end{aligned} \tag{A5}$$

for $\ell = 1, 2, \ldots, M$.

In what follows, we show the procedure of how to reduce the bilinear equation (A1) to the bilinear equation (3). The bilinear equations in Eq. (A1) are $(2 + M)$ dimensional and the bilinear equations in Eq. (3) are $(1 + 1)$ dimensional. So, we have to perform dimension reduction. To this end, we rewrite the tau function (A2) as

$$\tau_0 = \prod_{s=1}^{K} e^{\xi_s + \overline{\xi}_s} |m'_{s,j}|, \tag{A6}$$

where

$$m'_{s,j} = \frac{1}{p_s + \overline{p}_j} + \sum_{\ell=1}^{M} \frac{1}{q_s^{(\ell)} + \overline{q}_j^{(\ell)}} e^{\eta_s^{(\ell)} - \xi_s + \overline{\eta}_j^{(\ell)} - \overline{\xi}_j}. \tag{A7}$$

Since

$$\begin{aligned}&\left(\partial_{x_1} - \sum_{\ell=1}^{M} \delta_\ell \partial_{y_\ell}\right) m'_{s,j}\\ &\quad = \sum_{\ell=1}^{M} \left(\delta_\ell + \frac{p_s + \overline{p}_j}{q_s^{(\ell)} + \overline{q}_j^{(\ell)}}\right) e^{\eta_s^{(\ell)} - \xi_s + \overline{\eta}_j^{(\ell)} - \overline{\xi}_j},\end{aligned} \tag{A8}$$

and if the parameters p_s, q_s satisfy the following parameter constraints

$$q_s^{(\ell)} = -\frac{p_s}{\delta_\ell}, \quad \overline{q}_j^{(\ell)} = -\frac{\overline{p}_j}{\delta_\ell}, \tag{A9}$$

for $s, j = 1, 2, \ldots, K$ and $\ell = 1, 2, \ldots, M$, then one can obtain

$$\partial_{x_1} m'_{sj} = \sum_{\ell=1}^{M} \delta_\ell \partial_{y_\ell} m'_{s,j}. \tag{A10}$$

This leads to the following dimension reduction:

$$\partial_{x_1} \tau_0 = \sum_{\ell=1}^{M} \delta_\ell \partial_{y_\ell} \tau_0. \tag{A11}$$

Under the above dimension reduction, the bilinear equations in Eqs. (A1) give rise to the following bilinear equation:

$$D_{x_1}^2 \tau_0 \tau_0 = -2 \sum_{\ell=1}^{M} \delta_\ell \tau_1(\ell)\tau_{-1}(\ell). \tag{A12}$$

Therefore, under the parameter constraint (A9), the bilinear equations in Eqs. (A1) could reduce to the following bilinear equations:

$$\begin{aligned}0 &= \left(D_{x_1}^2 - D_{x_2}\right)\tau_1(\ell)\tau_0,\\ D_{x_1}^2 \tau_0 \tau_0 &= -2 \sum_{\ell=1}^{M} \delta_\ell \tau_1(\ell)\tau_{-1}(\ell).\end{aligned} \tag{A13}$$

The variable y_ℓ appearing in the tau functions given by Eq. (A2) satisfying the bilinear equations (A13) is a dummy variables and is chosen to be zero. By further assuming $x_1 = x$, $x_2 = it$, and taking $f = \tau_0$, $g^{(\ell)} = \tau_1(\ell)$, $g^*(-x,t) = -\tau_{-1}(\ell)$ when the tau functions of $2N \times 2N$ determinant form [i.,e., $K = 2N \times 2N$ in Eq. (A2)] satisfy the nonlocal symmetry reduction $\tau_0^*(-x,t) = \tau_0(x,t)$, $\tau_1^*(\ell)(-x,t) = -\tau_{-1}(\ell)(x,t)$. Also by taking $f = \tau_0$, $g^{(\ell)} = \tau_1(\ell)$, $g^*(-x,t) = \tau_{-1}(\ell)$ when the tau functions of $(2N+1) \times (2N+1)$ determinant form [i.e., $K = 2N+1 \times 2N+1$ in Eq. (A2)] satisfy the nonlocal symmetry reduction $\tau_0^*(-x,t) = -\tau_0(x,t)$, $\tau_1^*(\ell)(-x,t) = \tau_{-1}(\ell)(x,t)$. Then the tau functions defined in Eq. (A2) would reduce to the tau functions of the bilinear equations of nonlocal M-NLS equations (3), for these two choices which would generate, respectively, bright soliton solutions (6) to the nonlocal M-NLS equations (2) with zero or periodic line wave boundary conditions.

In the following step, we first perform the nonlocal symmetry reduction $\tau_0^*(-x,t) = \tau_0(x,t)$, $\tau_1^*(\ell)(-x,t) = -\tau_{-1}(\ell)(x,t)$ with variable transformations $x_1 = x$, $x_2 = it$. To this end, we consider $K = 2N \times 2N$ matrices for the tau functions τ_0, $\tau_1(\ell)$, and $\tau_{-1}(\ell)$ defined in Eq. (A2) and take the parameters satisfying the following constraint condition:

$$\begin{gathered} p_{N+s} = -p_s, \quad \overline{p}_{N+s} = -\overline{p}_s, \quad \overline{p}_s = p_s^*, \quad \overline{\xi}_{s,0} = \xi_{s,0}, \\ \overline{\eta}_{j,0}^{(\ell)} = \eta_{j,0}^{(\ell)}, \quad \xi_{N+s,0} = \xi_{s,0}^*, \quad \overline{\xi}_{N+s,0} = \overline{\xi}_{s,0}^*, \\ \eta_{N+s,0}^{(\ell)} = \eta_{j,0}^{(\ell)*}, \quad \overline{\eta}_{N+s,0}^{(\ell)} = \overline{\eta}_{j,0}^{(\ell)*}, \end{gathered} \tag{A14}$$

for $s = 1, 2, \ldots, N$. In this case, one can directly obtain

$$\begin{gathered} (\xi_s + \overline{\xi}_j)(x,t) = (p_s + p_j^*)x + i\left(p_s^2 - p_j^{*2}\right)t + 2\xi_{s,0}, \\ (\xi_{N+s} + \overline{\xi}_{N+j})(x,t) = -(p_s + p_j^*)x + i\left(p_s^{*2} - p_j^2\right)t + 2\xi_{s,0}^*, \\ \overline{\xi}_s(x,t) = p_s^* x - i p_s^* t + \xi_s, 0, \\ \xi_{N+s}(x,t) = -p_s x + i p_s^2 t + \xi_{s,0}^*, \end{gathered} \tag{A15}$$

which implies

$$\begin{gathered} (\xi_s + \overline{\xi}_j)^*(-x,t) = (\xi_{N+s} + \overline{\xi}_{N+j})(x,t), \\ \overline{\xi}_s^*(-x,t) = \xi_{N+s}(x,t). \end{gathered} \tag{A16}$$

Similarly,

$$\begin{gathered} (\xi_s + \overline{\xi}_{K+j})^*(-x,t) = (\xi_j + \overline{\xi}_{K+s})(x,t), \\ (\xi_{K+s} + \overline{\xi}_j)^*(-x,t) = (\xi_{K+j} + \overline{\xi}_s)(x,t), \\ (\xi_{K+j} + \overline{\xi}_{K+s})^*(-x,t) = (\xi_s + \overline{\xi}_j)(x,t), \\ \overline{\xi}_{N+s}(x,t) = \xi_s^*(-x,t). \end{gathered} \tag{A17}$$

Therefore,

$$\begin{gathered} m_{K+s,K+j}^*(-x,t) = -m_{j,s}(x,t), \\ m_{K+s,j}^*(-x,t) = -m_{K+j,s}(x,t), \\ m_{s,K+j}^*(-x,t) = -m_{j,K+s}(x,t), \\ m_{s,j}^*(-x,t) = -m_{K+j,K+s}(x,t), \end{gathered} \tag{A18}$$

which gives rise to

$$\begin{aligned} \tau_0^*(-x,t) &= \begin{vmatrix} m_{s,j}^*(-x,t) & m_{s,N+j}^*(-x,t) \\ m_{N+s,j}^*(-x,t) & m_{N+s,N+j}^*(-x,t) \end{vmatrix} \\ &= \begin{vmatrix} m_{N+s,N+j}^*(-x,t) & m_{N+s,j}^*(-x,t) \\ m_{s,N+j}^*(-x,t) & m_{s,j}^*(-x,t) \end{vmatrix} \\ &= (-1)^{2N} \begin{vmatrix} m_{j,s}(x,t) & m_{N+j,s}(x,t) \\ m_{j,N+s}(x,t) & m_{N+j,N+s}(x,t) \end{vmatrix} \\ &= \tau_0(x,t), \end{aligned} \tag{A19}$$

and

$$\begin{aligned} \tau_1^*(\ell)(-x,t) &= \begin{vmatrix} m_{s,j}^*(-x,t) & m_{s,N+j}^*(-x,t) & e^{\xi_s^*(-x,t)} \\ m_{N+s,j}^*(-x,t) & m_{N+s,N+j}^*(-x,t) & e^{\xi_{N+s}^*(-x,t)} \\ -e^{\overline{\eta}_j^{(\ell)*}} & -e^{\overline{\eta}_{N+j}^{(\ell)*}} & 0 \end{vmatrix} \\ &= \begin{vmatrix} m_{N+s,N+j}^*(-x,t) & m_{N+s,j}^*(-x,t) & e^{\xi_{N+s}^*(-x,t)} \\ m_{s,N+j}^*(-x,t) & m_{s,j}^*(-x,t) & e^{\xi_s^*(-x,t)} \\ -e^{\overline{\eta}_{N+j}^{(\ell)*}} & -e^{\overline{\eta}_j^{(\ell)*}} & 0 \end{vmatrix} \\ &= (-1)^{2N+1} \begin{vmatrix} m_{j,s}(x,t) & m_{N+j,s}(x,t) & -e^{\overline{\xi}_s(x,t)} \\ m_{j,N+s}(x,t) & m_{N+j,N+s}(x,t) & -e^{\overline{\xi}_{N+s}(x,t)} \\ e^{\eta_j^{(\ell)}} & e^{\eta_{N+j}^{(\ell)}} & 0 \end{vmatrix} \\ &= -\begin{vmatrix} m_{s,j}(x,t) & m_{s,N+j}(x,t) & e^{\eta_j^{(\ell)}} \\ m_{N+j,j}(x,t) & m_{N+j,N+j}(x,t) & e^{\eta_{N+j}^{(\ell)}} \\ -e^{\overline{\xi}_j(x,t)} & -e^{\overline{\xi}_{N+j}(x,t)} & 0 \end{vmatrix} \\ &= -\tau_{-1}(\ell)(x,t). \end{aligned} \tag{A20}$$

Hence the bilinear equations (A13) reduce to the bilinear equations (3) of the nonlocal M-NLS equation with $f = \tau_0$, $g^{(\ell)} = \tau_1^{(\ell)}$, $g^{(\ell)*}(-x,t) = -\tau_{-1}^{(\ell)}$, and $c = 1$. Then the tau functions defined in Eq. (A2) with variable transformations $x_1 = x$, $x_2 = it$ and under the parametric constraints in Eqs. (A9) and (A14) reduce to tau functions of the bilinear equations of the nonlocal M-NLS equations (3), which would generate bright soliton solutions (6) to the nonlocal M-NLS equations (2) with zero boundary condition.

Finally, we perform the nonlocal symmetry reduction $\tau_0^*(-x,t) = -\tau_0(x,t)$, $\tau_1^*(\ell)(-x,t) = \tau_{-1}(\ell)(x,t)$ with variable transformations $x_1 = x$, $x_2 = it$. Then, we consider $K = (2N+1)\times(2N+1)$ matrices for the tau functions τ_0, $\tau_1(\ell)$, and $\tau_{-1}(\ell)$ defined in Eq. (A2) and take some parameters meeting the constraint condition in Eq. (A14) and the remaining parameters following the parameter constraint condition

$$\begin{aligned} p_{2N+1} &= \overline{p}_{2N+1} = ip, \\ \overline{\xi}_{2N+1,0} &= \xi^*_{2N+1,0}, \\ \overline{\eta}^{(\ell)}_{2N+1,0} &= \eta^{(\ell)*}_{2N+1,0}. \end{aligned} \tag{A21}$$

Therefore, the matrix elements $m_{s,j}$ still verify the identities in Eq. (A18) for $s, j = 1, 2, \ldots, N$, and the remaining matrix elements $m_{2N+1,j}$, $m_{2N+1,N+j}$, $m_{N+s,2N+1}$, $m_{s,2N+1}$, and $m_{2N+1,2N+1}$ meet the following relations:

$$\begin{aligned} m^*_{2N+1,j}(-x,t) &= -m_{N+j,2N+1}(x,t), \\ m^*_{s,2N+1}(-x,t) &= -m_{2N+1,N+s}(x,t), \\ m^*_{2N+1,2N+1}(-x,t) &= -m_{2N+1,2N+1}(x,t), \end{aligned} \tag{A22}$$

similarly as Eqs. (A19) and (A20), one can obtain

$$\tau_0^*(-x,t) = -\tau_0(x,t), \quad \tau_1^*(\ell)(-x,t) = \tau_{-1}(\ell)(x,t). \tag{A23}$$

Hence the bilinear equations (A13) reduce to the bilinear equations (3) of the nonlocal M-NLS equation with $f = \tau_0$, $g^{(\ell)} = \tau_1^{(\ell)}$, $g^{(\ell)*}(-x,t) = \tau_{-1}^{(\ell)}$, $c = -1$, and the tau functions defined in Eq. (A2) with variable transformations $x_1 = x$, $x_2 = it$ and under the parameter constraints in Eqs. (A9) and (A21). Finally, the bright soliton solutions (6) to the nonlocal M-NLS equations (2) on the periodic line wave background are thus obtained.

[1] P. G. Kevrekidis, D. J. Frantzeskakis, and R. Carretero-González, *Emergent Nonlinear Phenomena in Bose-Einstein Condensates: Theory and Experiment* (Springer, Heidelberg, 2008); C. Pethick and H. Smith, *Bose-Einstein Condensation in Dilute Gases* (Cambridge University Press, United Kingdom, 2002).

[2] P. G. Kevrekidis and D. J. Frantzeskakis, Solitons in coupled nonlinear Schrödinger models: A survey of recent developments, Rev. Phys. **1**, 140 (2016).

[3] V. S. Bagnato, D. J. Frantzeskakis, P. G. Kevrekidis, B. A. Malomed, and D. Mihalache, Bose-Einstein condensation: Twenty years after, Rom. Rep. Phys. **67**, 5 (2015).

[4] E. P. Bashkin and A. V. Vagov, Instability and stratification of a two-component Bose-Einstein condensate in a trapped ultracold gas, Phys. Rev. B **56**, 6207 (1997).

[5] M. J. Abowitz and T. K. Horikis, Interacting nonlinear wave envelopes and rogue wave formation in deep water, Phys. Fluids **27**, 012107 (2015).

[6] Y. S. Kivshar and G. P. Agrawal, *Optical Solitons: From Fibers to Photonic Crystals* (Academic Press, San Diego, 2003).

[7] B. A. Malomed, D. Mihalache, F. Wise, and L. Torner, Spatiotemporal optical solitons, J. Opt. B: Quantum Semiclassical Opt. **7**, R53 (2005).

[8] B. A. Malomed and D. Mihalache, Nonlinear waves in optical and matter-wave media: A topical survey of recent theoretical and experimental results, Rom. J. Phys. **64**, 106 (2019).

[9] Y. V. Kartashov, G. E. Astrakharchik, B. A. Malomed, and L. Torner, Frontiers in multidimensional self-trapping of nonlinear fields and matter, Nat. Rev. Phys. **1**, 185 (2019).

[10] A. C. Scott, *Nonlinear Science: Emergence and Dynamics of Coherent Structures* (Oxford University Press, Oxford, 1999).

[11] H. Bailung and Y. Nakamura, Observation of modulational instability in a multi-component plasma with negative ions, J. Plasma Phys. **50**, 231 (1993); H. Bailung, S. K. Sharma, and Y. Nakamura, Observation of Peregrine Solitons in a Multicomponent Plasma with Negative Ions, Phys. Rev. Lett. **107**, 255005 (2011).

[12] G. P. Agrawal, *Nonlinear Fiber Optics* (Academic Press, New York, USA, 2013).

[13] N. Akhmediev and A. Ankiewicz, *Solitons: Nonlinear Pulses and Beams* (Chapman and Hall, London, 1997).

[14] R. Radhakrishnan, R. Sahadevan, and M. Lakshmanan, Integrability and singularity structure of coupled nonlinear Schrödinger equations, Chaos, Solitons Fractals **5**, 2315 (1995).

[15] V. G. Makhan'kov and O. K. Pashaev, Nonlinear Schrödinger equation with noncompact isogroup, Theor. Math. Phys. **53**, 979 (1982).

[16] D. N. Christodoulides and M. I. Carvalho, Bright, dark, and gray spatial soliton states in photorefractive media, J. Opt. Soc. Am. B **12**, 1628 (1995).

[17] T. H. Coskun, D. N. Christodoulides, M. Mitchell, and M. Segev, Theory of Incoherent Self-Focusing in Biased Photorefractive Media, Phys. Rev. Lett. **78**, 646 (1997).

[18] J. U. Kang, G. I. Stegeman, J. S. Aitchison, and N. Akhmediev, Observation of Manakov Spatial Solitons in AlGaAs Planar Waveguides, Phys. Rev. Lett. **76**, 3699 (1996); D. Rand, I. Glesk, C.-S. Brès, D. A. Nolan, X. Chen, J. Koh, J. W. Fleischer, K. Steiglitz, and P. R. Prucnal, Observation of Temporal Vector Soliton Propagation and Collision in Birefringent Fiber, *ibid.* **98**, 053902 (2007).

[19] B. Frisquet, B. Kibler, P. Morin, F. Baronio, M. Conforti, G. Millot, and S. Wabnitz, Polarization modulation instability in a Manakov fiber system, Sci. Rep. **6**, 20785 (2016).

[20] S. Chakravarty, M. J. Ablowitz, J. R. Sauer, and R. B. Jenkins, Multisoliton interactions and wavelength-division multiplexing, Opt. Lett. **20**, 136 (1995).

[21] C. Yeh and L. Bergman, Enhanced pulse compression in a nonlinear fiber by a wavelength division multiplexed optical pulse, Phys. Rev. E **57**, 2398 (1998).

[22] F. Poletti and P. Horak, Description of ultrashort pulse propagation in multimode optical fibers, J. Opt. Soc. Am. B **25**, 1645 (2008); A. Mecozzi, C. Antonelli, and M. Shtaif, Nonlinear propagation in multi–mode fibers in the strong coupling regime, Opt. Express **20**, 11673 (2012); S. Mumtaz, R. J. Essiambre, and G. P. Agrawal, Nonlinear propagation in multimode and multicore fibers: Generalization of the manakov equations, J. Lightwave Technol. **31**, 398 (2013).

[23] C. M. Bender and S. Boettcher, Real Spectra in Non-Hermitian Hamiltonians Having $\mathcal{PT}$ Symmetry, Phys. Rev. Lett. **80**, 5243 (1998).

[24] C. M. Bender, Introduction to $\mathcal{PT}$-symmetric quantum theory, Contemp. Phys. **46**, 277 (2005).

[25] R. El-Ganainy, K. G. Makris, D. N. Christodoulides, and Z. H. Musslimani, Theory of coupled optical $\mathcal{PT}$-symmetric structures, Opt. Lett. **32**, 2632 (2007).

[26] V. V. Konotop, J. Yang, and D. A. Zezyulin, Nonlinear waves in $\mathcal{PT}$-symmetric systems, Rev. Mod. Phys. **88**, 035002 (2016).

[27] C. E. Rüter, K. G. Markis, R. El-Ganainy, D. N. Christodoulides, M. Segev, and D. Kip, Observation of parity-time symmetry in optical systems, Nat. Phys. **6**, 192 (2010).

[28] B. Peng, S. K. Özdemir, F. Lei, F. Monifi, M. Gianfreda, G. L. Long, S. Fan, F. Nori, C. M. Bender, and L. Yang, Parity-time-symmetric whispering-gallery microcavities, Nat. Phys. **10**, 394 (2014).

[29] M. J. Ablowitz and Z. H. Musslimani, Integrable Nonlocal Nonlinear Schrödinger Equation, Phys. Rev. Lett. **110**, 064105 (2013).

[30] M. J. Ablowitz, D. J. Kaup, A. C. Newell, and H. Segur, The inverse scattering transform-Fourier analysis for nonlinear problems, Stud. Appl. Math. **53**, 249 (1974).

[31] M. J. Ablowitz and Z. H. Musslimani, Inverse scattering transform for the integrable nonlocal nonlinear Schrödinger equation, Nonlinearity **29**, 915 (2016).

[32] M. J. Ablowitz, X. D. Luo, and Z. H. Musslimani, Inverse scattering transform for the nonlocal nonlinear Schrödinger equation with nonzero boundary conditions, J. Math. Phys. **59**, 011501 (2018).

[33] M. J. Ablowitz, B. F. Feng, X. D. Luo, and Z. H. Musslimani, Reverse space-time nonlocal sine-Gordon/sinh-Gordon equations with nonzero boundary conditions, Stud. Appl. Math. **141**, 267 (2018).

[34] M. J. Ablowitz, B. F. Feng, X. D. Luo, and Z. H. Musslimani, Inverse scattering transform for the nonlocal reverse space-time nonlinear Schrödinger equation, Theor. Math. Phys. **196**, 1241 (2018).

[35] Y. Rybalko and D. Shepelsky, Long-time asymptotics for the integrable nonlocal nonlinear Schrödinger equation, J. Math. Phys. **60**, 031504 (2019).

[36] A. K. Sarma, M. A. Miri, Z. H. Musslimani, and D. N. Christodoulides, Continuous and discrete Schrödinger systems with parity-time-symmetric nonlinearities, Phys. Rev. E **89**, 052918 (2014).

[37] M. Li and T. Xu, Dark and antidark soliton interactions in the nonlocal nonlinear Schrödinger equation with the self-induced parity-time-symmetric potential, Phys. Rev. E **91**, 033202 (2015).

[38] M. Li, T. Xu, and D. X. Meng, Rational solitons in the parity-time-symmetric nonlocal nonlinear Schrödinger model, J. Phys. Soc. Jpn. **85**, 124001 (2016).

[39] Y. S. Zhang, D. Q. Qiu, Y. Cheng, and J. S. He, Rational solution of the nonlocal nonlinear Schrödinger equation and its application in optics, Rom. J. Phys. **62**, 108 (2017).

[40] S. K. Gupta and A. K. Sarma, Peregrine rogue wave dynamics in the continuous nonlinear Schrödinger system with parity-time symmetric Kerr nonlinearity, Commun. Nonlinear Sci. Numer. Simul. **36**, 141 (2016).

[41] S. K. Gupta, A string of Peregrine rogue waves in the nonlocal nonlinear Schrödinger equation with parity-time symmetric self-induced potential, Opt. Commun. **411**, 1 (2018).

[42] B. Yang and J. Yang, Rogue waves in the nonlocal $\mathcal{PT}$-symmetric nonlinear Schrödinger equation, Lett. Math. Phys. **109**, 945 (2019).

[43] J. Yang, General N-solitons and their dynamics in several nonlocal nonlinear Schrödinger equations, Phys. Lett. A **383**, 328 (2019).

[44] G. Q. Zhang, Z. Y. Yan, and Y. Chen, Novel higher-order rational solitons and dynamics of the defocusing integrable nonlocal nonlinear Schrödinger equation via the determinants, Appl. Math. Lett. **69**, 113 (2017).

[45] X. Y. Wen, Z. Y. Yan, and Y. Q. Yang, Dynamics of higher-order rational solitons for the nonlocal nonlinear Schrödinger equation with the self-induced parity-time-symmetric potential, Chaos **26**, 063123 (2016).

[46] M. Gürses and A. Pekcan, Nonlocal nonlinear Schrödinger equations and their soliton solutions, J. Math. Phys. **59**, 051501 (2018).

[47] A. Khare and A. Saxena, Periodic and hyperbolic soliton solutions of a number of nonlocal nonlinear equations, J. Math. Phys. **56**, 032104 (2015).

[48] K. Chen and D. J. Zhang, Solutions of the nonlocal nonlinear Schrödinger hierarchy via reduction, Appl. Math. Lett. **75**, 82 (2018).

[49] B. F. Feng, X. D. Luo, M. J. Ablowitz, and Z. H. Musslimani, General soliton solution to a nonlocal nonlinear Schrödinger equation with zero and nonzero boundary conditions, Nonlinearity **31**, 5385 (2018).

[50] X. Huang and L. M. Ling, Soliton solutions for the nonlocal nonlinear Schrödinger equation, Eur. Phys. J. Plus **131**, 148 (2016).

[51] J. G. Rao, Y. Cheng, K. Porsezian, D. Mihalache, and J. S. He, $\mathcal{PT}$-symmetric nonlocal Davey-Stewartson I equation: Soliton solutions with nonzero background, Phys. D **401**, 132180 (2020).

[52] B. Yang and J. Yang, Transformations between nonlocal and local integrable equations, Stud. Appl. Math. **140**, 178 (2018).

[53] T. A. Gadzhimuradov and A. M. Agalarov, Towards a gauge-equivalent magnetic structure of the nonlocal nonlinear Schrödinger equation, Phys. Rev. A **93**, 062124 (2016).

[54] M. J. Ablowitz and Z. H. Musslimani, Integrable nonlocal nonlinear equations, Stud. Appl. Math. **139**, 7 (2017).

[55] A. S. Fokas, Integrable multidimensional versions of the nonlocal nonlinear Schrödinger equation, Nonlinearity **29**, 319 (2016).

[56] J. Yang, Physically significant nonlocal nonlinear Schrödinger equation and its soliton solutions, Phys. Rev. E **98**, 042202 (2018).
[57] C. Menyuk, Pulse propagation in an elliptically birefringent Kerr media, IEEE J. Quantum Electron. **25**, 2674 (1989).
[58] A. Mecozzi, C. Antonelli, and M. Shtaif, Coupled Manakov equations in multimode fibers with strongly coupled groups of modes, Opt. Express, **20**, 23436 (2012).
[59] X. Li and X. Xie, Improving cooling performance of the mechanical resonator with the two-level-system defects, Phys. Rev. A **90**, 033804 (2014).
[60] I. V. Barashenkov, S. V. Suchkov, A. A. Sukhorukov, S. V. Dmitriev, and Y. S. Kivshar, Breathers in $\mathcal{PT}$-symmetric optical couplers, Phys. Rev. A **86**, 053809 (2012).
[61] Y. V. Bludov, R. Driben, V. V. Konotop, and B. A. Malomed, Instabilities, solitons and rogue waves in $\mathcal{PT}$-coupled nonlinear waveguides, J. Opt. (Bristol, U. K.) **15**, 064010 (2013).
[62] R. Driben and B. A. Malomed, Stability of solitons in parity-time-symmetric couplers, Opt. Lett. **36**, 4323 (2011).
[63] D. Nath, Y. Gao, R. Babu Mareeswaran, T. Kanna, and B. Roy, Bright-dark and dark-dark solitons in coupled nonlinear Schrödinger equation with $\mathcal{PT}$-symmetric potentials, Chaos **27**, 123102 (2017).
[64] A. J. Martínez, M. I. Molina, S. K. Turitsyn, and Y. S. Kivshar, Violation of Bell's inequality for phase-singular beams, Phys. Rev. A **91**, 023822 (2015).
[65] M. Gürses, Nonlocal Fordy-Kulish System on Symmetric Spaces, Phys. Lett. A **381**, 1791 (2017).
[66] A. P. Fordy and P. P. Kulish, Nonlinear Schrödinger equations and simple Lie algebras, Commun. Math. Phys. **89**, 427 (1983).
[67] D. Sinha and P. K. Ghosh, Integrable nonlocal vector nonlinear Schrödinger equation with self-induced parity-time-symmetric potential, Phys. Lett. A **381**, 124 (2017).
[68] H. Zhang, M. Zhang, and R. Hu, Darboux transformation and soliton solutions in the parity-time-symmetric nonlocal vector nonlinear Schrödinger equation, Appl. Math. Lett. **76**, 170 (2018).
[69] G. Zhang and Z. Yan, Multi-rational and semi–rational solitons and interactions for the nonlocal coupled nonlinear Schrödinger equations, Europhys. Lett. **118**, 60004 (2017).
[70] Y. Zhang, Y. Liu, and X. Tang, A general integrable three-component coupled nonlocal nonlinear Schrödinger equation, Nonlinear Dyn. **89**, 2729 (2017).
[71] S. Stalin, M. Senthilvelan, and M. Lakshmanan, Degenerate soliton solutions and their dynamics in the nonlocal Manakov system: I symmetry preserving and symmetry breaking solutions, Nonlinear Dyn. **95**, 1767 (2019).
[72] S. Stalin, M. Senthilvelan, and M. Lakshmanan, Energy-sharing collisions and the dynamics of degenerate solitons in the nonlocal Manakov system, Nonlinear Dyn. **95**, 343 (2019).
[73] V. Matveev, Generalized Wronskian formula for solutions of the KdV equations: First applications, Phys. Lett. A **166**, 205 (1992).
[74] V. Matveev, Asymptotics of the multi-positon-soliton τ function of the Korteweg-de Vries equation and the supertransparency, J. Math. Phys. **35**, 2955 (1994).
[75] R. Beutler, Positon solutions of the sine-Gordon equation, J. Math. Phys. **34**, 3098 (1993).
[76] M. Jaworski and J. Zagrodzinski, Positon and positon-like solutions of the Korteweg-de Vries and sine-Gordon equations, Chaos, Solitons Fractals **5**, 2229 (1995).
[77] C. Rasinariu, U. Sukhatme, and A. Khare, Negaton and positon solutions of the KdV and mKdV hierarchy, J. Phys. A: Math. Gen. **29**, 1803 (1996).
[78] K. W. Chow, W. C. Lai, C. K. Shek, and K. Tso, Positon-like solutions of nonlinear evolution equations in $(2+1)$-dimensions, Chaos, Solitons Fractals **9**, 1901 (1998).
[79] W. C. Lai and K. W. Chow, 'Positon' and 'dromion' solutions of the $(2+1)$-dimensional long wave-short wave resonance interaction equations, J. Phys. Soc. Jpn. **68**, 1847 (1999).
[80] D. J. Zhang, Notes on solutions in Wronskian form to soliton equations: KdV-type, arXiv:nlin/0603008v3.
[81] D. J. Zhang, S. L. Zhao, Y. Y. Sun, and J. Zhou, Solutions to the modified Korteweg-de Vries equation, Rev. Math. Phys. **26**, 1430006 (2014).
[82] R. Hirota, *The Direct Method in Soliton Theory* (Cambridge University Press, Cambridge, 2004).
[83] B. Feng, General N-soliton solution to a vector nonlinear Schrödinger equation, J. Phys. A: Math. Theor. **47**, 355203 (2014).
[84] M. Sato, Soliton equations as dynamical systems on a infinite dimensional Grassmann manifolds, RIMS Kokyuroku **439**, 30 (1981).
[85] M. Jimbo and T. Miwa, Solitons and infinite dimensional lie algebras, Publ. Res. Inst. Math. Sci., Prepr. **19**, 943 (1983).
[86] E. Date, M. Kashiwara, M. Jimbo, and T. Miwa, Transformation Groups for Soliton Equations, in *Nonlinear Integrable Systems-Classical Theory and Quantum Theory*, edited by M. Jimbo and T. Miwa (World Scientific, Singapore, 1983), pp. 39–119.